Universität Stuttgart
Geodätisches Institut

GeoForschungsZentrum Potsdam
GPS/GALILEO-Technologien

Preprocessing of high rate GPS data for real-time applications

Diplomarbeit im Studiengang

Geodäsie und Geoinformatik

an der Universität Stuttgart

Zhiguo Deng

Stuttgart, April 2008

Betreuer:

Univ.Prof. Dr.phil.nat Markus Rothacher
GeoForschungsZentrum Potsdam

Dr. Maorong Ge
GeoForschungsZentrum Potsdam

Prüfer:

Prof. Dr.-Ing. Nico Sneeuw
Universität Stuttgart

Selbstständigkeitserklärung

Hiermit erkläre ich, Zhiguo Deng, dass ich die von mir eingereichte Diplomarbeit zum Thema

Preprocessing of high rate GPS data for real-time applications

selbstständig verfasst und ausschließlich die angegebenen Hilfsmittel und Quellen verwendet habe.

Datum, Ort: _____

Unterschrift: _____

(Zhiguo Deng)

Acknowledgements

Here I would like to express my sincere gratitude towards my supervisor Univ.Prof. Dr.phil.nat Markus Rothacher, who offered me the excellent opportunity to write my thesis at the section GPS/GALILEO-Technologien, GeoForschungsZentrum Potsdam. And I thank sincerely my professor Dr.-Ing. Nico Sneeuw, head of Institute of Geodesy at Universität Stuttgart, for his patience and supervision.

My sincere appreciation is conveyed to my distinguished supervisor Dr. Maorong Ge for his continuous guidance, discussions and helpful advice throughout my studies. And my thanks also go to my friends: Dr. Markus Vennebus, Dr. Junping Chen and Dipl. Michal Dähnn for their encouragement and comments.

I give my very special thanks to my dear parents for providing me upbringing and education. Their encouragements helped me finishing my diploma study in Germany. There are also numerous people, their great support and helpfulness gave me strength to follow the path I have chosen.

Table of contents

List of figures

List of tables

Zusammenfassung

In den letzten Jahren immer mehr geodätische Anwendungen erforderten GPS Daten mit 1 Hz sampling rate, zum Beispiel die Low Earth Orbiter Missionen CHAMP und GRACE sowie GPS Überwachungsnetze. In der gleichen Zeit verbesserten die wachsenden Kapazitäten des Internets den Transport von Daten in Echtzeit und die langfristige Archivierung mit weniger Kosten. Dies erfordert GPS Software mit der Fähigkeit GPS-Daten und-Netze in Echtzeit zu verarbeiten. Weil nur ein Cycle Slip die GPS-Lösung verfälschen kann, ist das Preprocessing von GPS Daten besonders wichtig für die Erhaltung der hohen Genauigkeit.

Zurzeit gibt es eine ganze Reihe von verfügbaren Techniken für diesen Zweck. In dieser Arbeit wird ein neuer Algorithmus vorgestellt, mit dem Cycle Slip von 1 Hz GPS Daten in Echtzeit erkannt werden können. Um die Verarbeitung der 1 Hz GPS Daten in Echtzeit zu gewährleisten, muss der neue Algorithmus schnell und voll-automatisch arbeiten. Desweteren müssen die Verfügbarkeit, Zuverlässigkeit und Effektivität auch berücksichtigt werden. Nach dem Studium der 1Hz GPS Daten und existierende Algorithmen wird ein neuer Algorithmus in dieser Arbeit entwickelt. Der Algorithmus verwendet Differenzen zwischen Satellitenträgerphasen und ionosphärische (geometriefreie) lineare Kombination. Mit Polynom Fitting werden cycle slips gesucht.

In dieser Arbeit wird die Leistung des Algorithmus zur Bestimmung von Cycle Slips als Funktion von Satellitenelevationswinkeln, anhand Einzelfrequenzenempfänern wie Garmin, Thales und Notvale untersucht.

Schlüsselwörter:

- Cycle-Slip-Detektion in Echtzeit
- Real-Time GPS
- Polynom Fitting
- Ionosphärische Linearkombination
- Einzelfrequenzempfängern

Abstract

In the past several years, ever more geodetic applications require GPS data with 1-Hz sampling rate, for example, the Low Earth Orbiter missions CHAMP and GRACE GPS monitoring networks. In the same time, the growing capacities of the Internet allowed improvements in the real-time transport of data and long-term archiving became less expensive. This requires GPS software with the capability to deal with real-time GPS data and networks. To obtain high accuracy GPS solution the GPS carrier phase measurements are used. Since even a single cycle slip in GPS carrier phase measurements significantly falsifies GPS solutions, the GPS preprocessing is very important for maintaining the high accuracy.

Currently there are quite a number of available techniques for the pre-processing. But to process high rate GPS data in real time the new algorithm must be able to run in real-time and fully automatically. At the same time the availability, reliability and efficiency must be also taken into account. After studying high rate GPS data and existing algorithm, a new algorithm is developed in this thesis. The algorithm uses single differences between-satellite carrier phases and ionospheric combination (geometry-free linear combination), and applies polynomial fitting to detect cycle slips.

In this thesis the performance of the algorithm will be investigated as a function of satellite elevation angles and the utility of the cycle slip detection for single frequency receivers Garmin, Thales and Novatel is investigated.

Key words:

- Cycle-slip detection in real time
- Real time GPS
- Polynomial fitting
- Ionosphere combination
- Single frequency receiver

1. Introduction

1.1 Motivation

An earthquake is the result of a sudden release of energy in the Earth's crust that creates seismic waves. In 2004 an earthquake in the Indian ocean triggered a series of devastating tsunamis along the coasts of most landmasses bordering the Indian Ocean, killing more than 225,000 people in eleven countries and staggering total of economic damage to US$ 103 billion [Wikipedia]. With the support of Federal Ministry of Education and Research (Germany) a new project GPS calls GSEIS (SurfacE Deformations withIn Seconds) began in Section 1.1 GeoForschungsZentrum Potsdam (GFZ) on April 1st 2007. The project GSEIS focuses on development and test a system for real-time monitoring of the Earth's surface using GPS/GNSS (Global Navigation Satellite System) technique. Its objective is monitoring effectively earthquakes and volcanic eruptions with the help of satellite remote sensing.

Most of the GPS monitoring systems process data daily or hourly to achieve station coordinates with a precision of a few millimeters. However, in early warning systems the time lag between a natural hazard event and issue of the warning must be as short as possible. In order to quickly estimate the scale of an ongoing rupture GPS data should be streamed via a network, processed in near-real or real-time and integrated with the seismic observations. The importance of the real-time approach should not be underestimated. The real-time strategy is of great significance for warning of volcano eruption, earthquake and tsunami disasters. It has been demonstrated already that dense high-rate GPS networks can measure large dynamic and static surface-ground motions with latencies of only few seconds. Thus, further development of real-time processing strategies and software applications in dense high-rate (1-Hz or higher) GPS networks is urgently needed. [Proposal GSEIS]

Before estimating parameters the received GPS data must be cleared from outliers and cycle slips. An important task of the GPS data pre-processing is the detection and possible correction of cycle slips.

1.2 Objective

In this thesis we concentrate on the preprocessing of 1 Hz GPS data for real time applications. Because of the increasing number of GPS stations in GPS networks it is becom-

ing difficult to run the preprocessing by one central computer in real time. To make the preprocessing more effective the received GPS data can be checked before it is sent from the GPS observing sites to an analyze central. Currently the most cycle slip detection algorithms are based on double- or triple-difference, and they are not able to realize single GPS station data preprocessing. In Blewitt (1990) the undifferenced cycle slip detection and fixing, called TurboEdit, was introduced. In this algorithm the ionospheric and wide-lane combinations are used for cycle slip detection; but since pseudorange are less precise than carrier phase, it confuses cycle slips with noise in wide-lane combinations. The pseudorange measurements in 1 Hz high rate GPS data have larger noise than that in lower rate GPS data.

In this work the TurboEdit algorithm is introduced, after the analysis of 1 Hz GPS data a new strategy is discussed for single GPS station preprocessing in real time.

1.3 Real-time GPS

Today double differencing GPS for accurate positioning is the most common data preprocessing method, because common modes errors such as satellite orbital errors, receiver clock errors, satellite clock errors and atmospheric delay can be reduced for long baselines or even eliminated for short baselines. And after double differencing the double difference ambiguities are constrained to integer values.

Currently carrier phase based GPS kinematic positioning systems are primarily based on double differencing data processing approach which is able to provide centimeter to decimeter accurate positional accuracy in real time. [Gao, Y et al. 2004]

During the last 10 years the availability of precise GPS satellite orbit and clock products of the International GPS Service (IGS) has enabled the development of the new positioning methodology ‘precise point positioning’ (PPP). In PPP the pseudorange and carrier phase observations from a single GPS receiver are undifferenced. The reference receiver is not necessary any more. To compare with DGPS it is logistically simpler and almost as accurate. [Witchayangkoon, B. 2002]

In 2002 the IGS Real-time Working Group (RTWG) was founded to be aimed to the IGS developing real-time infrastructure and processes. The GFZ Potsdam is one of participating agencies of the RTWG. A prototype system will be developed in GFZ Potsdam for the support of precise real-time positioning. The primary products of such a system will be GPS/GNSS station data and satellite orbits and clocks, made available to the user by Internet and other streaming technologies.

Chapter 1 Introduction

At present an increasing number of GPS stations can provide real-time data streams. Therefore appropriate corresponding software packages are needed. A related software package, as a prototype of the future real-time GNSS software at GFZ, has been developed recently for both real-time deformation monitoring and providing service for applications based on PPP under the framework of GSEIS project.

The real-time software packages for GSEIS will be capable of

- Providing satellite orbits and clocks in real-time (network solution).
- Kinematic monitoring of station positions in real-time for networks with good real-time data transmission.
- Performing real-time PPP for stations in high-rate data communications based on orbit and clocks from the network solution (in such cases only orbits and clocks have to be transferred to the station). [Rothacher, M et al. proposal GSEIS 2003]

2. Background

Before estimating the parameter (of e.g. station coordinates, receiver clock error etc.) in GPS processing, the observations must be cleaned with the preprocessing. In the preprocessing step poor phase observations are marked. There are quite a number of available techniques for this purpose. In this chapter the definition of cycle slips and several linear combinations will be introduced, which are always used for cycle slips detection. At last part of this chapter the automatic editing algorithm for undifferenced GPS data [Blewitt 1990], called TurboEdit, will be discussed.

2.1 Cycle Slips

Carrier phase measurements contain an unknown integer number *b* of cycles called ambiguity. This integer number has to be identified in order to exploit the full accuracy potential of GPS carrier phase measurements. During the carrier phase measurements, referenced to the first phase measurement the ambiguity can be continued only when the receiver maintains lock on the received GPS signal. But in some situations, the receiver looses lock of the phase lock loop which might be due to poor signal reception; very fast acceleration changes, or shadowing of satellite signals in their path. Such situations cause discontinuities in the phase measurements, called cycle slips. [Keller, W 2005]

Cycle slips can be any size ranging from one to millions of cycles and can occur concurrently and differently on L1 and L2. After a cycle slip a new ambiguity must be re-estimated. There are lots of methods for cycle slips detection such as triple-difference and TurboEdit [Blewitt 1990]. For cycle slip detection usually the observation combinations and differences are applied. In combinations and differences many errors can be eliminated. Invariably a few cycle slips remain undetected, requiring analyst intervention to fully clean up the data.

2.2 Function Model and Definitions

Both the carrier phase and pseudorange observables are used for the PPP method. The following GPS carrier phase and pseudorange equations on two carriers L_1 and L_2 are expressed in units of distance.

$$\Phi_1 = \rho - \frac{If_2^2}{f_1^2 - f_2^2} + \lambda_1 b_1 \tag{2.1a}$$

$$\Phi_2 = \rho - \frac{If_1^2}{f_1^2 - f_2^2} + \lambda_2 b_2 \tag{2.1b}$$

$$P_1 = \rho + \frac{If_1^2}{f_1^2 - f_2^2} \tag{2.1c}$$

$$P_2 = \rho + \frac{If_2^2}{f_1^2 - f_2^2} \tag{2.1d}$$

Φ_1 Φ_2 : measured carrier phase scaled to distance (meters) on carriers L_1 and L_2

P_1 P_2 : P Code Pseudoranges on carrier L_1 and L_2

f_1 f_2 : carrier frequencies

λ_1 λ_2 : carrier wavelengths

ρ : non-dispersive delay (included geometric delay, troposphere delay, clock signatures and identical effects on carrier L_1 and L_2)

I : ionospheric delay parameter

b_1 b_2 : phase ambiguities $b \in Z$

GPS satellites transmit two carriers, f_1 = 10.23 MHz × 154 = 1575.42 MHz (wavelength $\lambda_1 \approx$ 19.0 cm) and f_2 = 10.23 MHz × 120 = 1227.6 MHz (wavelength $\lambda_2 \approx$ 24.4 cm). On the carriers two codes are modulated, a precision (P) code (on both carriers phase L_1 & L_2), and a coarse acquisition code C/A (only on L_1).

For ease of discussion, some terms are ignored in the equations, like data noise, multipath, phase center effects, and higher order ionospheric effects.

2.3 Linear combination of data

Linear combinations and differences of data are very useful, since some errors can be eliminated by combinations and differences. Here three combinations and one difference are introduced.

- Wide-lane Combination
- Ionospheric Combination (geometry-free linear combination)
- Ionosphere-free Combination (ionosphere-free linear combination)
- Single difference between satellites (one receiver and two satellites)

The test data for graphical visualization of the combinations and differences is sampled from the IGS station PIE1 in Pie Town (USA JPL), the sampling rate is 30 seconds. A H-MASER provides the standard frequency. In doy 260 year 2007, the first 3 hours observations from PRN 9 are used.

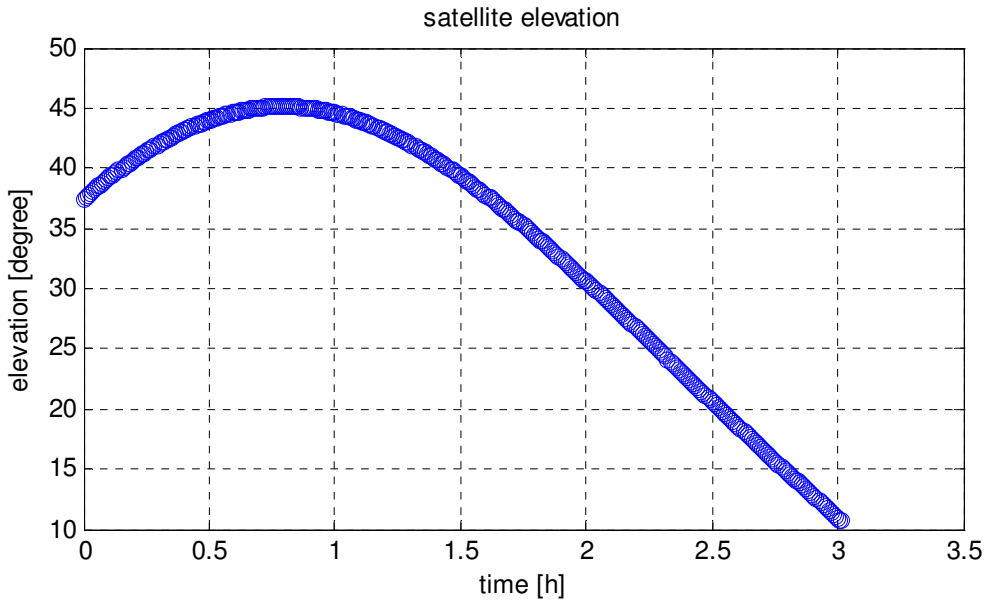

Figure 2.1 Satellite elevation

Because cycle slips can occur concurrently and differently on L_1 and L_2, each signal must be processed independently to check for cycle slips. For these purpose two linear combinations from the equations (2.1a-d) observations can be chosen for cycle slip detection.

2.3.1 Wide-Lane phase combination

The wide-lane phase combination and its phase delay and pseudorange can be written:

$$\Phi_{\mathrm{w}} = \frac{f_1\Phi_1 - f_2\Phi_2}{f_1 - f_2} = \rho + \frac{If_1f_2}{f_1^2 - f_2^2} + \lambda_w b_w \tag{2.2a}$$

$$P_{\mathrm{w}} = \frac{f_1P_1 + f_2P_2}{f_1 + f_2} = \rho + \frac{If_1f_2}{f_1^2 - f_2^2} \tag{2.2b}$$

Φ_{w} : wide-lane phase expressed as ranges

P_{w} : wide-lane pseudorange

b_{w} : wide-lane phase ambiguity $b_{\mathrm{w}} \equiv b_1 - b_2 \;\; b_{\mathrm{w}} \in \mathrm{Z}$

λ_{w} : wide-lane wavelength $\lambda_{\mathrm{w}} \equiv c/(f_1 - f_2) \approx 86.2$ cm

Because the wide-lane wavelength λ_{w} is very large, and the noise in the wide-lane pseudorange P_{w} is in decimeter level, Φ_{w} can be calibrated by P_{w}. From equations (2.2a-b) wide-lane ambiguity b_{w} can be presented from pseudorange and carrier phase observation as:

$$b_{\mathrm{w}} = \frac{L_{\mathrm{w}} - P_{\mathrm{w}}}{\lambda_{\mathrm{w}}} \tag{2.2c}$$

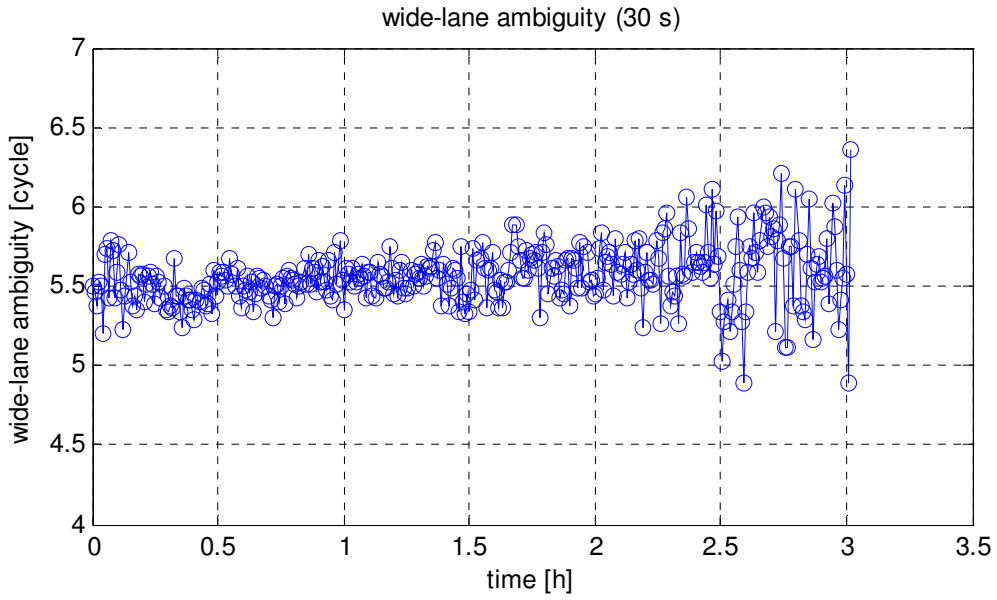

Figure 2.2 Wide-lane ambiguity

Theoretically, b_w should be constant. Due to multipath and other noise, the wide-lane ambiguity in Figure 2.2 has a variation between 5 and 6. When b_w in epoch i has a variation bigger than a given threshold, it is very likely, that a cycle slip has occurred. To find out on which signal the slip is happened, other combination is needed. Here the ionospheric combination (the geometry-free linear combination) is used.

2.3.2 Ionospheric combination

The ionospheric delay on GPS signals is frequency-dependent, i.e. the effect on the signal is different on the L_1 and L_2 signals. The ionospheric delay is a function of the latitude of the receiver, the season, the time of day, and the level of solar activity.

The Global Positioning System (GPS) transmits two frequencies, allowing users to correct for the first-order ionospheric signal group delay (or phase advance) that can be as large as 100 meters on L_1 frequency. The second-order ionospheric term, caused by the Faraday rotation effect induced by the Earth magnetic field, is about 1000 times smaller and usually ignored. [Kedar, S et al. 2004]

The ionospheric combination for carrier phase observation is:

$$\Phi_I \equiv \Phi_1 - \Phi_2 = I + \lambda_1 b_1 - \lambda_2 b_2 = I + \lambda_1 b_\delta - \lambda_I b_2 \tag{2.3a}$$

$$P_I \equiv P_2 - P_1 = I \tag{2.3b}$$

$$b_\delta = b_1 - b_2 \tag{2.3c}$$

Φ_I : ionospheric combination carrier phases expressed as ranges

P_I : ionospheric combination Pseudorange

b_σ : ionospheric combination ambiguity $b_\sigma \in Z$

λ_I : ionospheric combination wavelength $\lambda_I \equiv \lambda_2 - \lambda_1 \approx 5.4$ cm

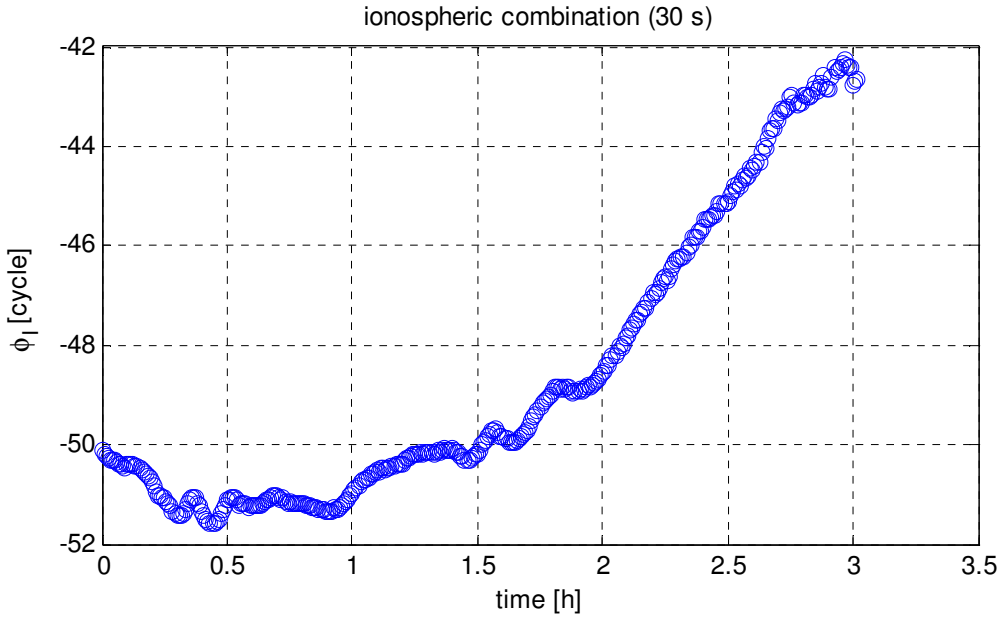

Figure 2.3 Ionospheric combination

The pseudorange P_I is a reasonably smooth function, but because sometimes the multi-path effect is bigger than the centimeter level, and the ionospheric combination wavelength is about 5.4 cm, is littler than the wide-lane combination wavelength 86.2 cm, Φ_I cannot be successfully calibrated by P_I like Φ_w.

It is possible to construct a polynomial fit Q to P_I and subtract it from Φ_I, then look for discontinuities as cycle slip. But under high ionospheric activity conditions it is difficult to detect slip with the ionospheric combination, even with high sampling rate.

2.3.3 Ionosphere-free combination

The particular ionosphere-free code combination is used on dual-frequency measurements to estimate the first order of the ionospheric delay. For single-frequency receivers it is not possible to account for this ionospheric delay in this way.

The ionosphere-free combinations for codes and phases are defined by:

$$\Phi_c \equiv (f_1^2\Phi_1 - f_2^2\Phi_2)/(f_1^2 - f_2^2) = \rho + \lambda_c b_c \quad (2.4a)$$

$$P_c = (f_1^2 P_1 - f_2^2 P_2)/(f_1^2 - f_2^2) \quad (2.4b)$$

$$b_c = b_1 - f_2 b_2 / f_1 \quad (2.4c)$$

$$\lambda_c = f_1 c/(f_1^2 - f_2^2) \approx 48.4\,\text{cm} \quad (2.4d)$$

Φ_c : the ionospheric-free combination carrier phases expressed as ranges

P_c : the ionospheric-free combination pseudorange

b_c : ionospheric-free combination ambiguity

λ_c : ionospheric-free combination wavelength

In the ionospheric-free combination the ambiguity term b_c is not an integer value any more.

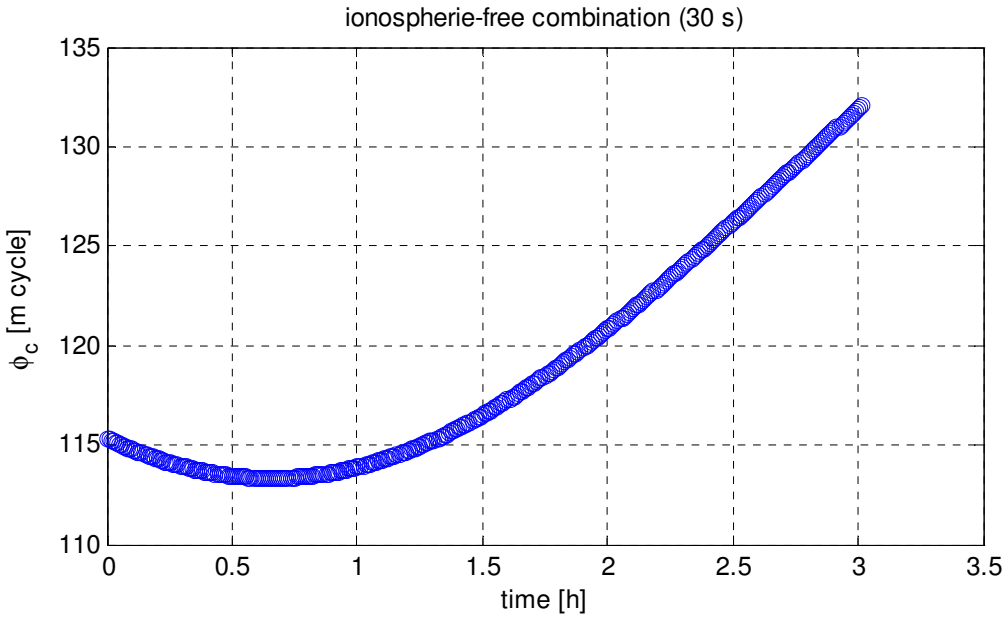

Figure 2.4 Ionosphere-free combination

From Figures 2.3 and 2.4 it can be seen, that the values of the ionospheric combination in the 3 hours change less than the values of ionosphere-free combination. But ionosphere-free combination looks like much smoother.

2.3.4 Differences between Satellites

For single stations, a useful function for slip detection is the between-satellite single difference (one receiver and two satellites) of carrier phases; it can be presented:

$$d\Phi_1^{m-n} \equiv \Phi_1^m - \Phi_1^n = \rho^{m-n} - \frac{I^{m-n} f_2^2}{f_1^2 - f_2^2} + \lambda_1 b_1^{m-n} \tag{2.5a}$$

$$d\Phi_2^{m-n} \equiv \Phi_2^m - \Phi_2^n = \rho^{m-n} - \frac{I^{m-n} f_1^2}{f_1^2 - f_2^2} + \lambda_2 b_2^{m-n} \tag{2.5b}$$

$d\Phi$: the phase difference between two satellite m, n

m, n : the satellites indices

The equations (2.5) are free of the receiver clock error. After the discontinuation of SA (selective availability) by The White House at 4.00 UTC on May 2, 2000, the biggest error source in GPS measurement is the receiver clock. The differences between satellites cancel the receiver clock error.

2.4 Cycle slip detection in TurboEdit

In 1989 Blewitt has developed an automatic editing algorithm for GPS data for undifferenced cycle slip detection and fixing. In the TurboEdit two linear combinations of the observations are used: the wide-lane combination and the ionospheric combination.

2.4.1 Cycle slip detection with the wide-lane combination

At every observation epoch TurboEdit calculates the wide-lane ambiguity b_w with equation (2.2c). In addition Blewitt gave a recursive algorithm to update sequentially the wide-lane ambiguity and its variance. For the variance an a priori RMS of half wide-lane cycles is set.

The formulae for the mean value of the wide-lane ambiguity $< b_w >$ and its variance σ is given by:

$$< b_w >_i = < b_w >_{i-1} + \frac{1}{i}(b_{w,i} - < b_w >_{i-1}) \tag{2.6a}$$

$$\sigma_i^2 = \sigma_{i-1}^2 + \frac{1}{i}\left[(b_{w,i} - < b_w >_{i-1})^2 - \sigma_{i-1}^2\right] \tag{2.6b}$$

$< b_w >$: mean value of the wide-lane ambiguity b_w

σ : variance of the wide-lane ambiguity b_w

i : epoch index in a continued data arc

In equation (2.6a) the mean is calculated exactly; the σ in the equation (2.6b) is an approximation, with a diminishing error term of $O(1 / i^2)$.

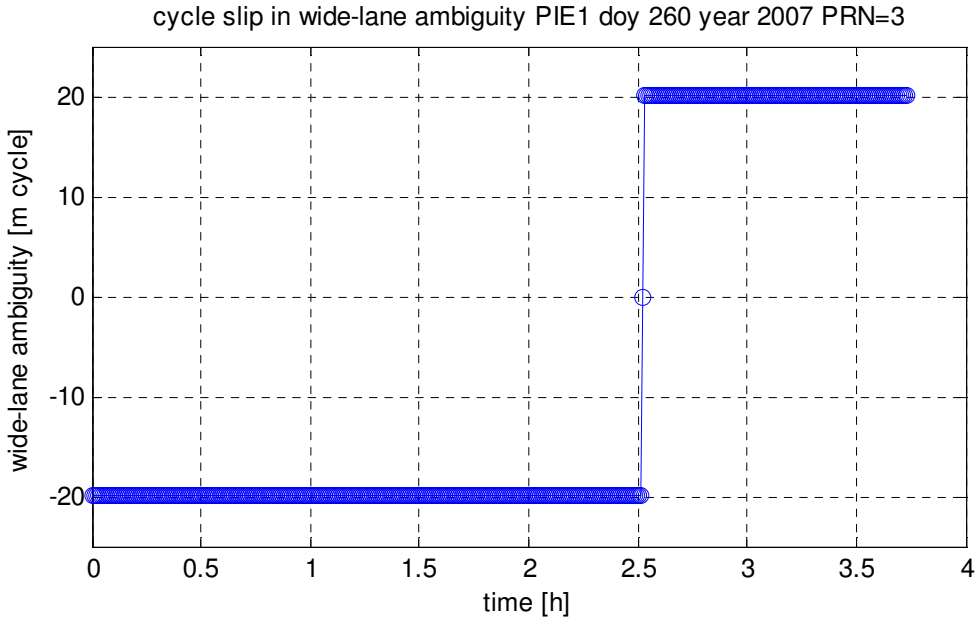

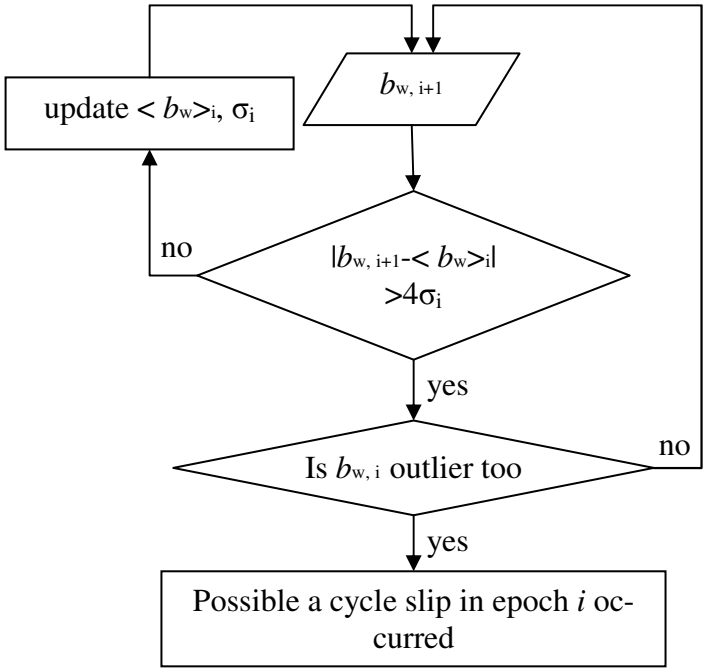

Figure 2.5 Cycle slip detection with wide-lane combination

After cycle slip the ambiguity changes to a different integer value, and it begin with a new < b_w>$_i$. When b_w of two continued epoch checked out as outliers, it is very possible a cycle slip occurred.

2.4.2 Cycle slip detection in the ionospheric combination

In the extremely unlikely case that the cycle slip in L_1 equals the one in L_2, then the wide-lane slip detection can not detect the cycle slip. In this case the ionospheric combination is used for cycle slip detection.

From equation (2.3b) it can be seen that the ionospheric pseudorange combination P_I is a reasonably smooth function, but because the multipath in pseudorange measurement is very often bigger than 10 cm, and Φ_I's wavelength is about 5.4cm. Φ_I can not be calibrated by P_I. To calibrate Φ_I a polynomial Q is fitted to P_I and then subtracted from Φ_I. The residuals are searched for discontinuities as outliers or cycle slips.

To choose the degree m of polynomial fit Blewitt suggested an empirical formula:

$$m = \min[(N/100+1),6] \tag{2.7a}$$

N : number of observations in the data

For detection of discontinuity in (L_I - Q) the algorithm is:

$$(L_{I,i} - Q_i) - (L_{I,i-1} - Q_{i-1}) > k \text{ cycle} \tag{2.7b}$$

$$(L_{I,i+1} - Q_{i+1}) - (L_{I,i} - Q_i) < 1 \text{ cycle} \tag{2.7c}$$

i : epoch index

k : threshold, default value is 6

When the above equations (2.7b) and (2.7c) are satisfied, then the epoch i is the first good data epoch point after the occurrence of a cycle slip.

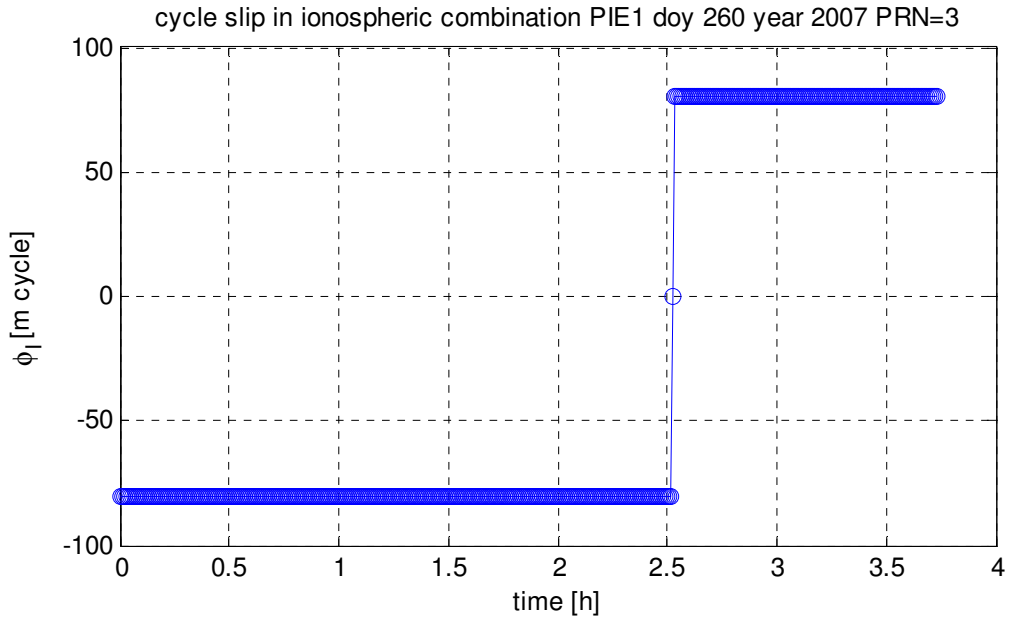

Figure 2.6 Cycle slip detection with ionospheric combination

Because of ionospheric activity for receivers at high latitudes and most cycle slip bigger than 6, Blewitt suggests: the default value of k is set to 6 ionospheric cycles (6 x 5.4 cm = 32.4 cm), but the threshold can be set to a more appropriate value depending on the ionospheric conditions.

However, there is a hidden problem in the ionospheric carrier phase combination for certain slip combinations. For example, a 24-cycles slip in L_1 and a 19-cycles slip in L_2 cause no jump in the ionospheric phase combination.

3. Preprocessing in EPOS

In the latest version of the EPOS (Earth Parameter & Orbit System) [Ge,M. et al. 2005] the preprocessing module "TB_Clean" is base on the algorithm TurboEdit. The implementation of Blewitt's algorithm TurboEdit in TB_Clean is introduced and some improvements are discussed.

3.1 Program flowchart

The TB-Clean is written in Fortran 90. The input files are observation files and navigation files in RINEX format. In the process of TB-Clean all measurements are ticked. To simplify the later parameters estimation the continued epochs longer than 5 minutes are used.

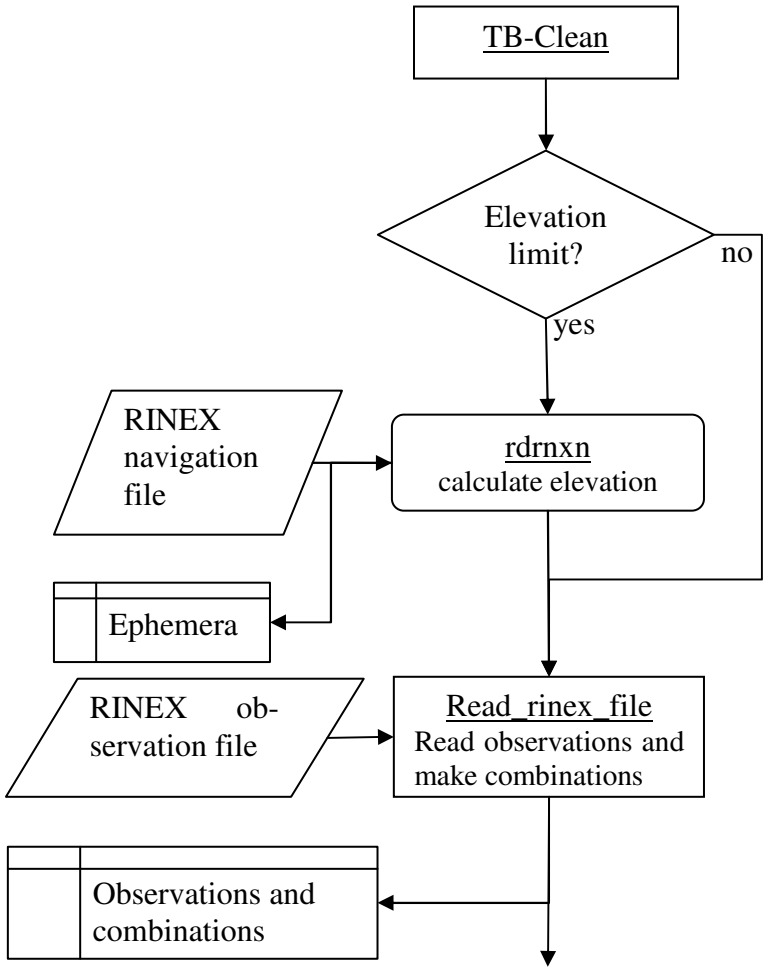

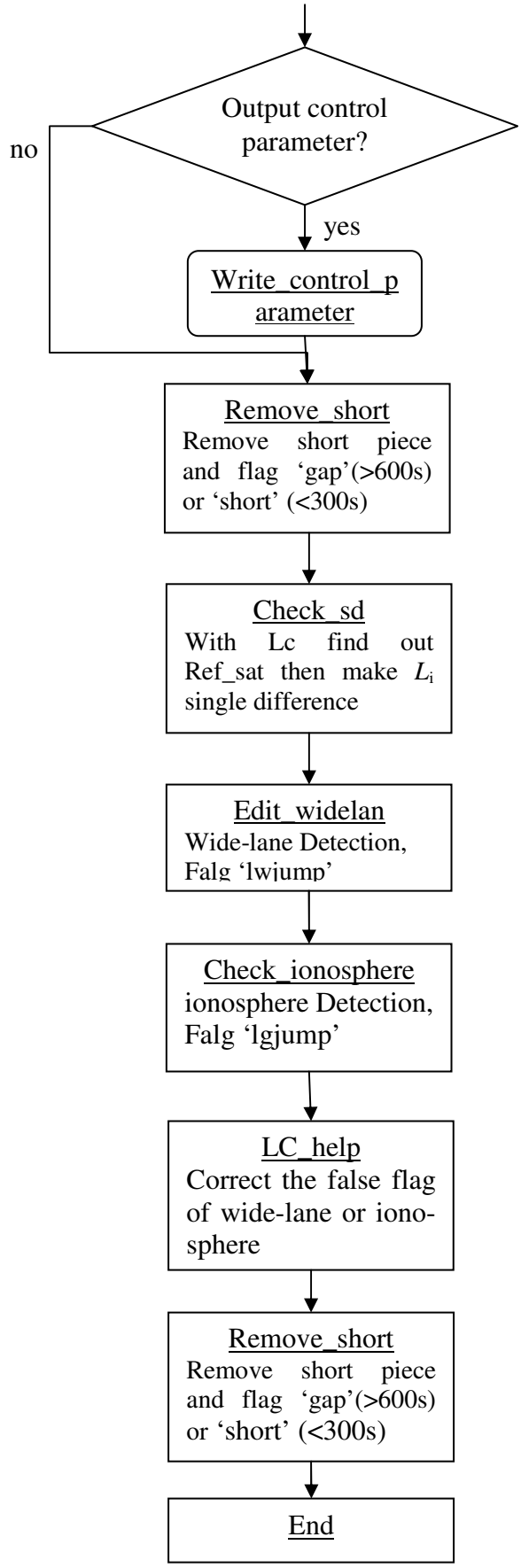

Figure 3.1 Program diagram of TB_Clean

3.2 Some difference between TurboEdit and TB_Clean

The thresholds in the program TB_Clean are different from those given by Blewitt. As Blewitt published TurboEdit in 1990, the SA (Selective Availability) technique was still active, the SA can introduce intentional, slowly changing random errors of up to a hundred meters into the publicly available navigation signals to confound. After the SA was terminated on May 1, 2000, the single difference between satellites is possible to be used to detect cycle slips and outliers. In TB_Clean there single difference between satellites ionospheric-free combination is used to detect cycle slips and it is very effective to deal with high ionosphere activity.

a) Threshold for wide-lane phase cycle slips detection.

In the cycle slip detection in the wide-lane combination of Blewitt if $|b_{w,\,i+1} - \langle b_w \rangle_i| > 4\sigma_i$, then the epoch i+1 observation is considered as a cycle slips. From the formulae for the wide-lane ambiguity b_w we know, that the ambiguity b_w should be a constant in a arc, when there is no cycle slip. If a cycle slips happens in L_1 or L_2, theoretically it should appear a same cycle slips by wide-lane ambiguity. In the subroutine TB_Clean the limit value is set as 1 cycle, one Wide-Lane wave length is about 86.2 cm. And a more condition is given: the jump between wide-lane ambiguities in two continued epochs should be smaller than half cycle. $|b_{w,\,i+1} - b_{w,\,i}| < 0.5$ cycle, about 43.1 cm. This condition requires the observations more smooth.

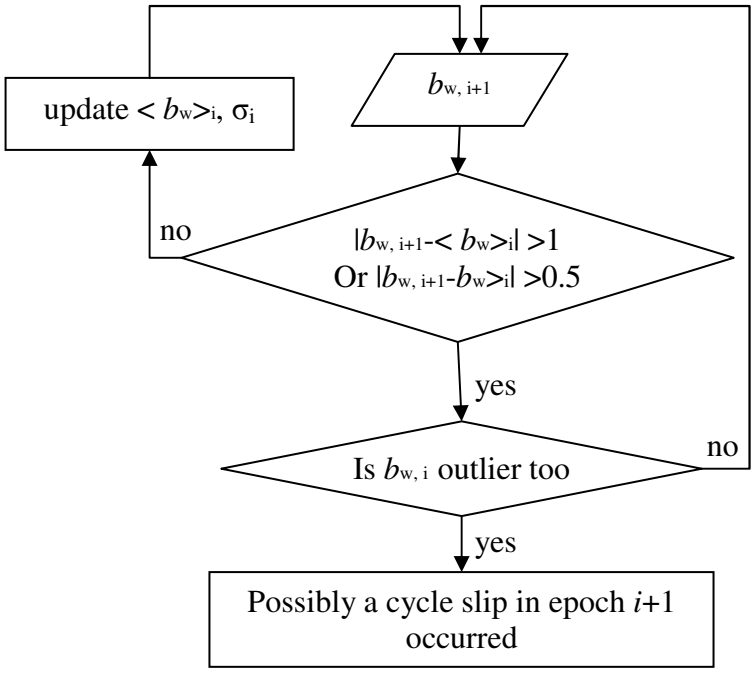

Figure 3.2 Cycle slip detection with wide-lane in TB_Clean

b) Ionospheric phase combination cycle slip detection

For the degree *m* of polynomial fit Q of the ionospheric combination is declared with the empirical equation (2.7a) by Blewitt.

But usually a quadratic polynomial fit is enough to deal with normal ionospheric activity; therefore in the subroutine TB_Clean the polynomial fit has no more than 2 degrees.

c) With single difference between in ionosphere-free phase combination

Blewitt also remarks, that under conditions of high ionospheric activity, the ionosphere-free combinations are a good choice for cycle slip detection. But unfortunately the ionosphere-free combinations is very sensitive to clock variations, most clocks of normal GPS receiver have this shortcoming. Then he suggested that it is also effective to difference the ionosphere-free combinations data between satellites.

Because the velocity of GPS satellite is very large, the ionosphere-free phase combinations increases or decreases also very quickly, for polynomial fitting it is not easy to find out small cycle slip. To avoid this situation the ionosphere-free phase combination is subtracted from the distance, which can be calculated from GPS broadcast ephemeris and approximate receiver position.

With the ionosphere-free combinations in continued 20 epochs a reference satellite is found out, which has most availed data in the 20 epochs and has a small RMS by a 2 degrees polynomial fit. Then after subtraction of satellite-receiver distance the ionosphere-free combinations of the other satellites are differenced with the reference satellite in these 20 epochs. After the fitting the big discontinuities are flagged as 'bigsd' (big jump in single difference).

Subroutine name:	**Used combination**	**Flag for possible cycle slip**
edit_widelane	Wide-Lane Combination	'lwjump'
check_ionosphere	Ionospheric Combination	'lgjump'
check_sd	Ionosphere-free Combination	'bigsd'

Table 3. 1 Used flags in TB_Clean

d) After the three combinations detection the subroutine 'LC_help' in TB_Clean compare with all flags, and make decision whether the tested epoch includes cycle slips. If the epoch has only one flag of 'lwjump' or 'lgjump', but without flag 'bigsd', then all flags of the epoch are cleared. This means, the epoch is accepted as a normal epoch without cycle slips.

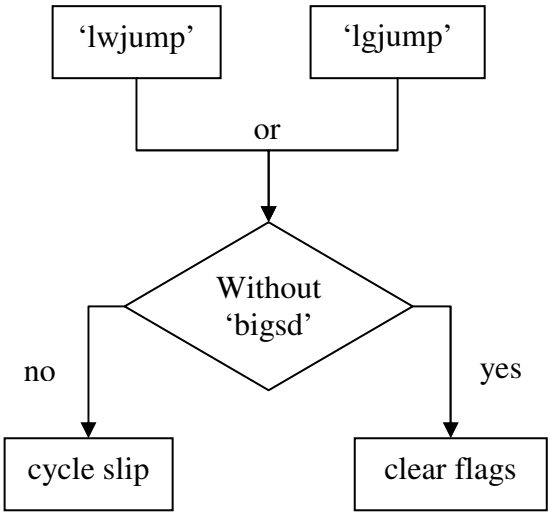

Figure 3.3 Compare all detections in subroutine 'LC_help'

3.3 Limitation in TB_Clean to deal with real-time GPS data

In the subroutine TB_Clean to detect cycle slip the polynomial fitting is applied. And the observations not only before and also after the test epoch are used to make the polynomial fitting. For real-time data, it is impossible to use the data after current epoch. Therefore the TB_Clean must be adapted to deal with real-time data, or a new method should be developed.

4. Compare 1 Hz and 0.033 Hz GPS data

Although many GPS receivers can operate at 1 to 10 Hz, most GPS measurements are sampled at 0.033 Hz. In the past several years, a growing number of continuous operating GPS receivers have increased their recording rates to 1 Hz. The high rate GPS data is beginning to be used for a variety of geophysical monitoring purposes, including seismology, missions in low Earth orbit. All above applications required 1 Hz GPS data processing in real time.

As improvement of the estimates of high-rate GPS position get more precise, the value of these high rate GPS monitoring systems become more important. In this chapter the differences of combinations for 1 Hz GPS data and 0.033 Hz GPS data are discussed, and a new data analysis's is proposed to detect cycle slip.

4.1 Real time 1 Hz GPS streaming data

Ntrip (Networked Transport of RTCM via Internet Protocol) is a procedure developed by Bundesamt für Kartographie und Geodäsie (BKG, Frankfurt am Main) and University of Dortmund to provide GNSS correction data as streaming data via the Internet. NTRIP is base on other streaming data procedures, for e. g. Internet Radio. [VermKV (Vermessungs- und Katasterverwaltung Rheinland-Pfalz)]

Using the NTRIP data streaming technology, raw data of globally distributed GNSS stations is retrieved from the BKG Ntrip Client by BKG, and are used for the estimation of both satellite clocks for PPP and station positions in network mode. The results are validated with IGS final products and with known station positions.

The project GSEIS gets real time 1 Hz GPS streaming data with the NTRIP data streaming technology. And our preprocessing should to process the streaming data.

4.2 Linear combinations in 1 Hz GPS data

Here the linear combinations in 1 Hz GPS data are compared with the linear combination in 0.033 Hz GPS data.

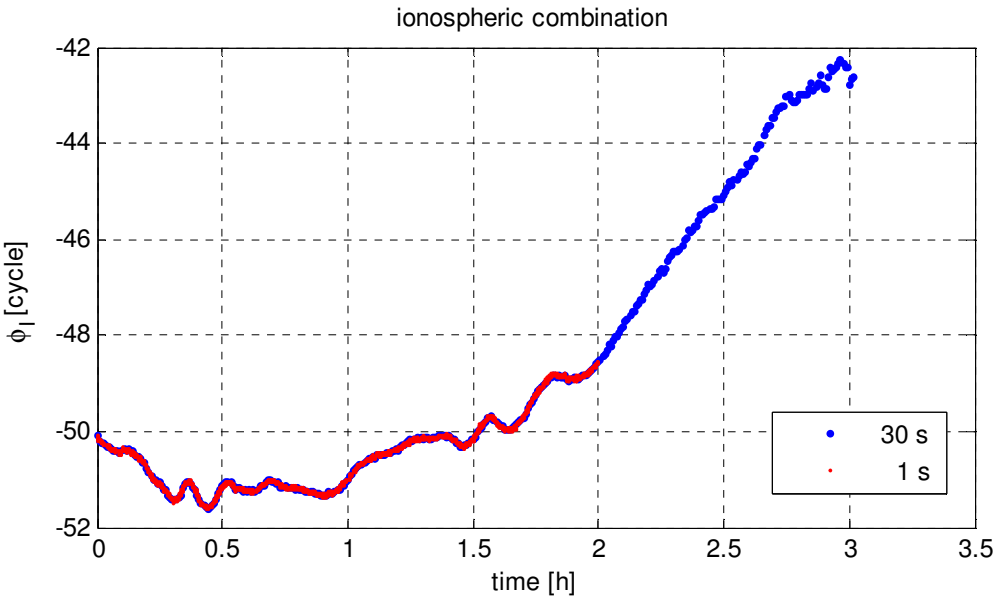

Figure 4.1 Ionospheric combinations of 1 Hz and 0.033 Hz

The Figure 4.1 shows us, that there is no difference in ionospheric combination between 1 Hz GPS data and 0.033 Hz. The ionospheric combination can be used to detect cycle slip. But some time because of high ionosphere activity the line is not smooth; in this case it can be difficult for polynomial fitting with low degree.

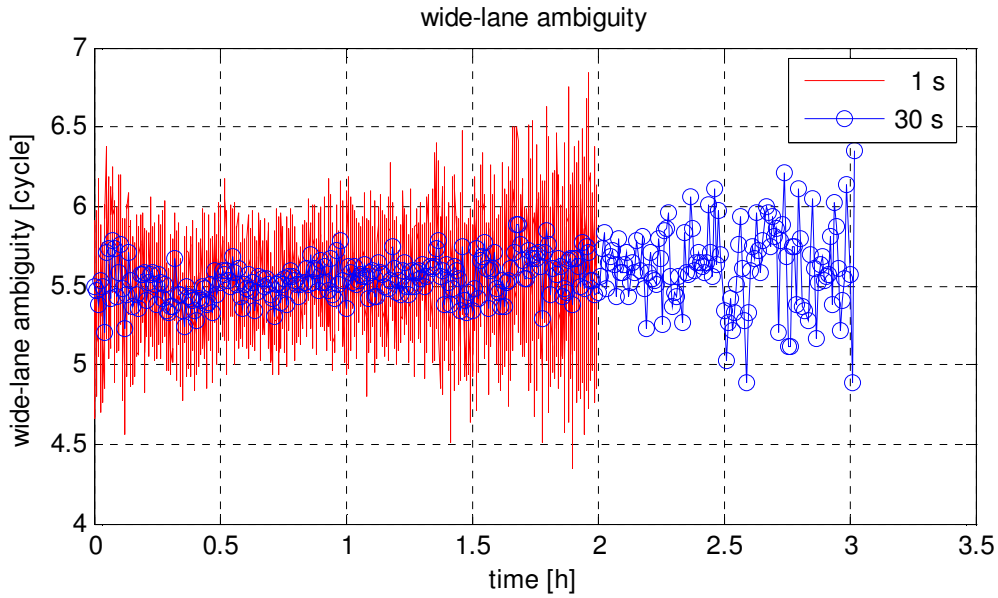

Figure 4. 2 Wide-lane ambiguities of 1 Hz and 0.033 Hz

From the identification of ionospheric combination's and the wide lane ambiguity's definition it can be seen, that in Figure 4.2 the bigger variations of 1 Hz wide lane ambiguity should come from the noise of pseudorange measurement. And it is too big to be used for cycle slip detection.

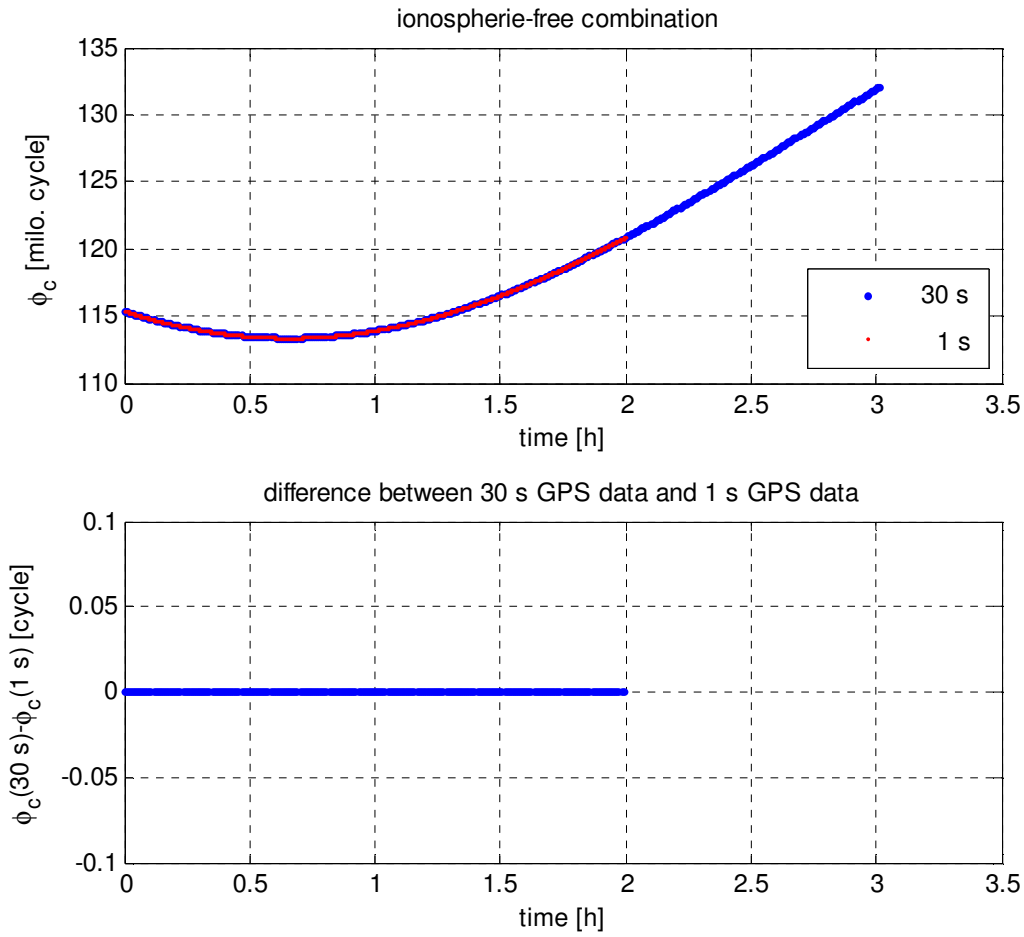

Figure 4. 3 Ionosphere-free combinations of 1 Hz and 0.033 Hz

The Figure 4.3 confirms again, that the 1 Hz GPS data sampling has same carrier phase measurements as 0.033 Hz GPS data.

As explained in chapter 3, because the velocity of GPS satellite is very large, for effective polynomial fitting of the ionosphere-free phase combination the distance between satellite and receiver should be subtracted, which can be calculated from GPS broadcast ephemeris and approximate receiver position. And the distance is calculated iteratively. For real-time PPP preprocessing purpose algorithm with iterations should be avoided.

4.3 1Hz GPS data problem of three IGS stations

Now about 110 sites of the IGS network can sample and send 1 Hz GPS data. 6 days' GPS data are downloaded. During the test it could be observed, that the IGS stations, POTM in Potsdam, WUH2 in Wuhan and OBE2 in Oberpfaffenhofen, have problems by sampling 1 Hz high-rate GPS data. As shown in the Figure 4.4 to 4.5.

The combinations oscillate at a frequency of about 0.25 Hz.

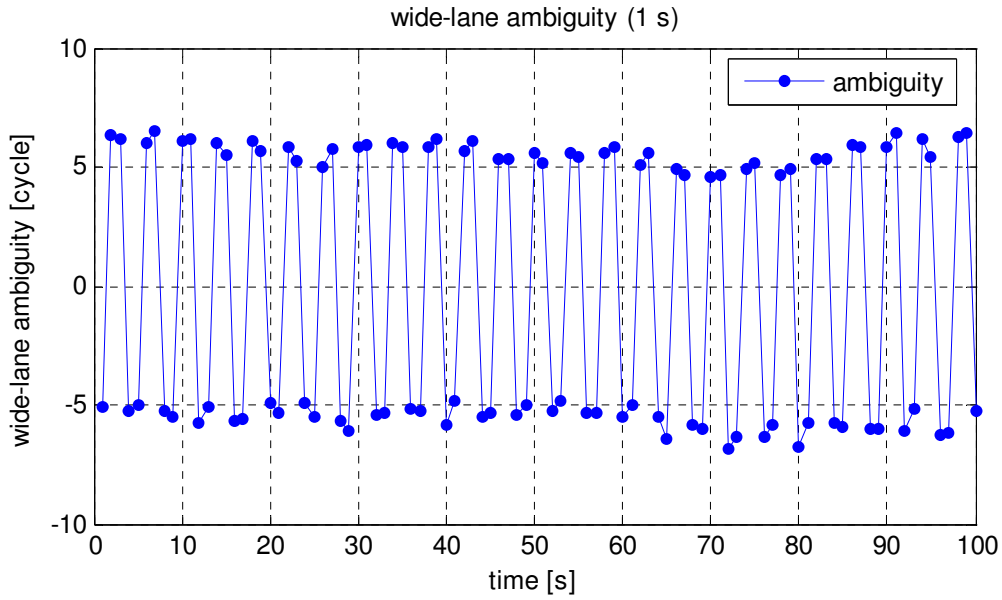

Figure 4. 4 Wide-lane ambiguities of 1Hz (data from WUH2, doy 260 year 2007 PRN3)

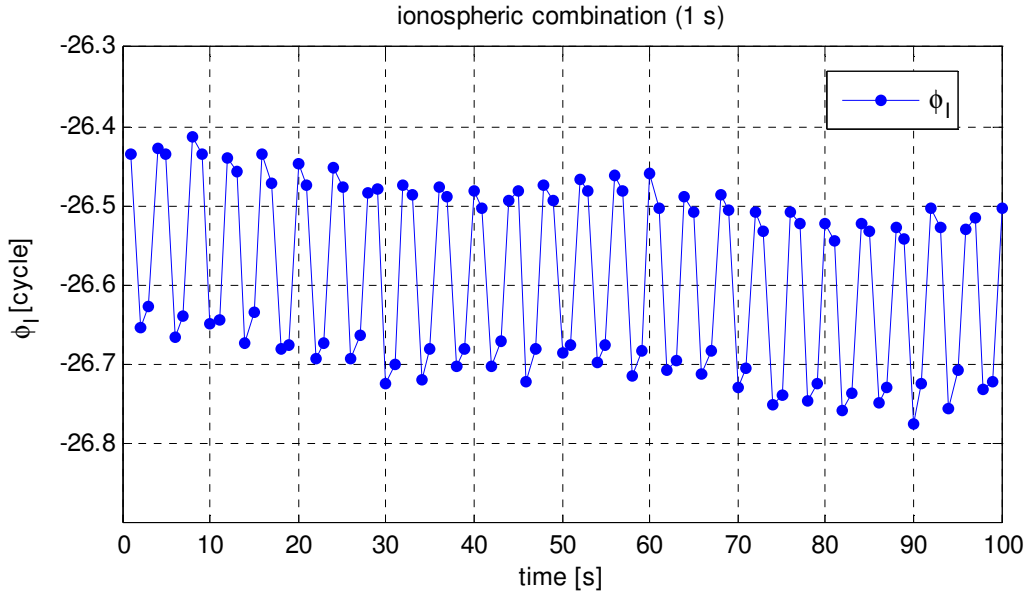

Figure 4. 5 Ionospheric combinations of 1 Hz (data from WUH2, doy 260 year 2007 PRN3)

From the equation (2.3) we know that the ionospheric combination is linear combination from L_1 and L_2, i.e. one or both of received signals L_1 and L_2 were not correctly generated by the GPS receiver.

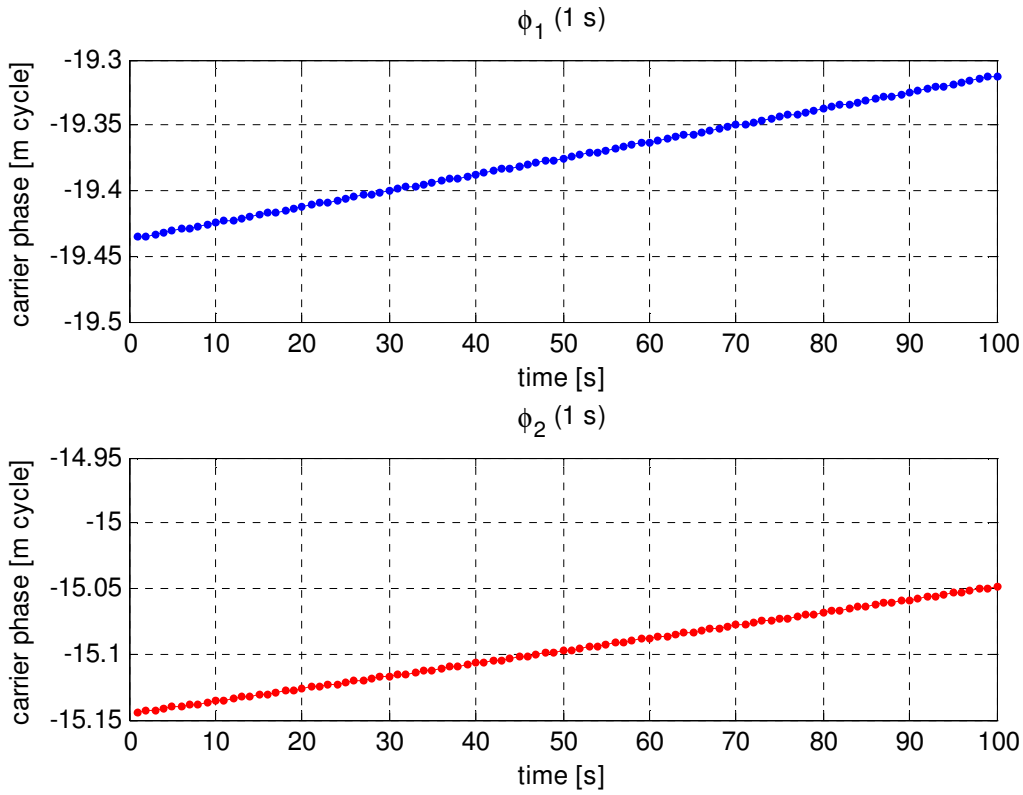

Figure 4. 6 Carrier phase Φ_1 and Φ_2 of 1Hz (data from WUH2, doy 260 year 2007 PRN3)

Because the GPS satellites have very high velocity, the carrier phase measurements increase rapidly. In the ionospheric- and wide lane combinations the geometric parts are cancelled, but there are also disadvantages, that the noise of the both the carrier phase measurements are enlarged.

Alone from the above four figures it is not clearly, which carrier phase measurements of WUH2 station causes the oscillation in the ionospheric combination and in wide lane combination.

The relative motion between GPS satellites and site receiver can be approximated by a constant acceleration motion.

Because of the high increase in the carrier phase we can not check the spectrum of the carrier phase Φ_1 and Φ_2 directly. Instead of the carrier phase Φ_1 and Φ_2 their second derivative are used to check the spectrum.

$$x_P(t) = \frac{A_0}{2} + \sum (A_k \cos k\omega_0 t + B_k \sin k\omega_0 t);\ k \le K \tag{3.1a}$$

$$x_P(t)'' = -\omega_0^2 \sum (A_k \cos k\omega_0 t + B_k \sin k\omega_0 t);\ k \le K \tag{3.1b}$$

$$x_P(t) = \frac{A_0}{2} - \frac{x_P(t)''}{\omega_0^2} \tag{3.1c}$$

From discrete Fourier transform form (3.1a-c) we know, the derivative of Φ_1 or Φ_2 maintain their frequency information.

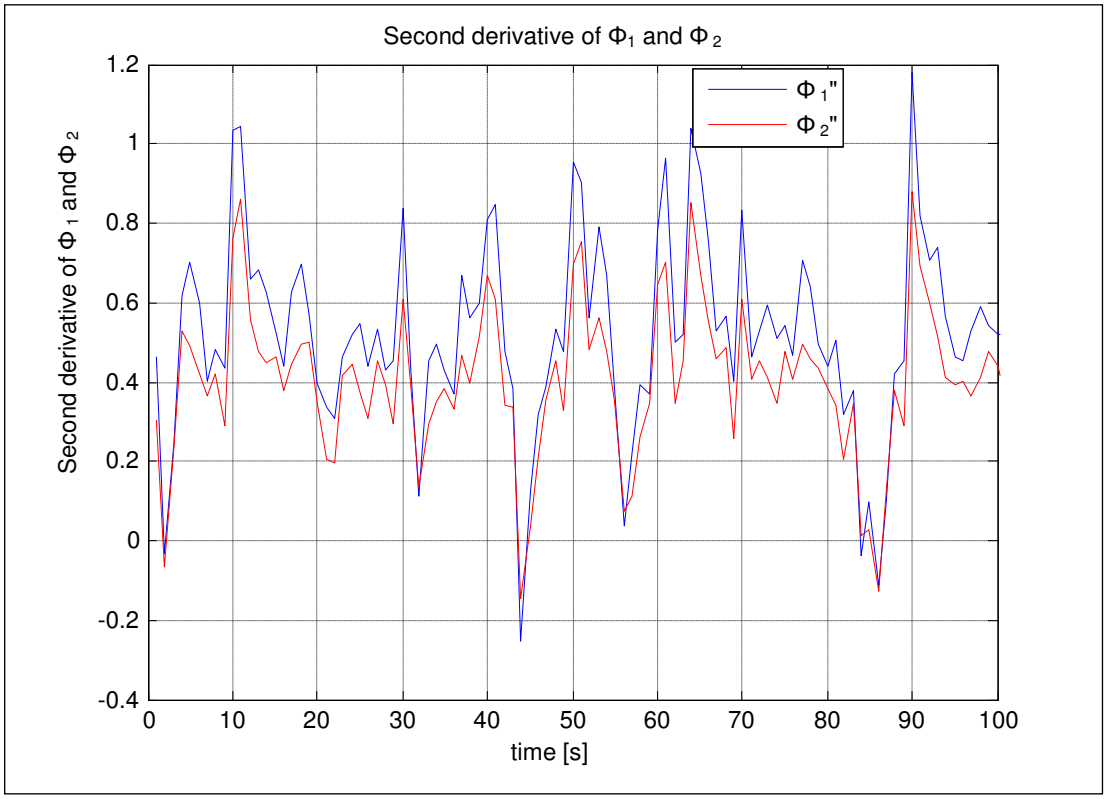

Figure 4. 7 Second derivative of Φ_1 and Φ_2 (data from WUH2, doy 260 year 2007 PRN3)

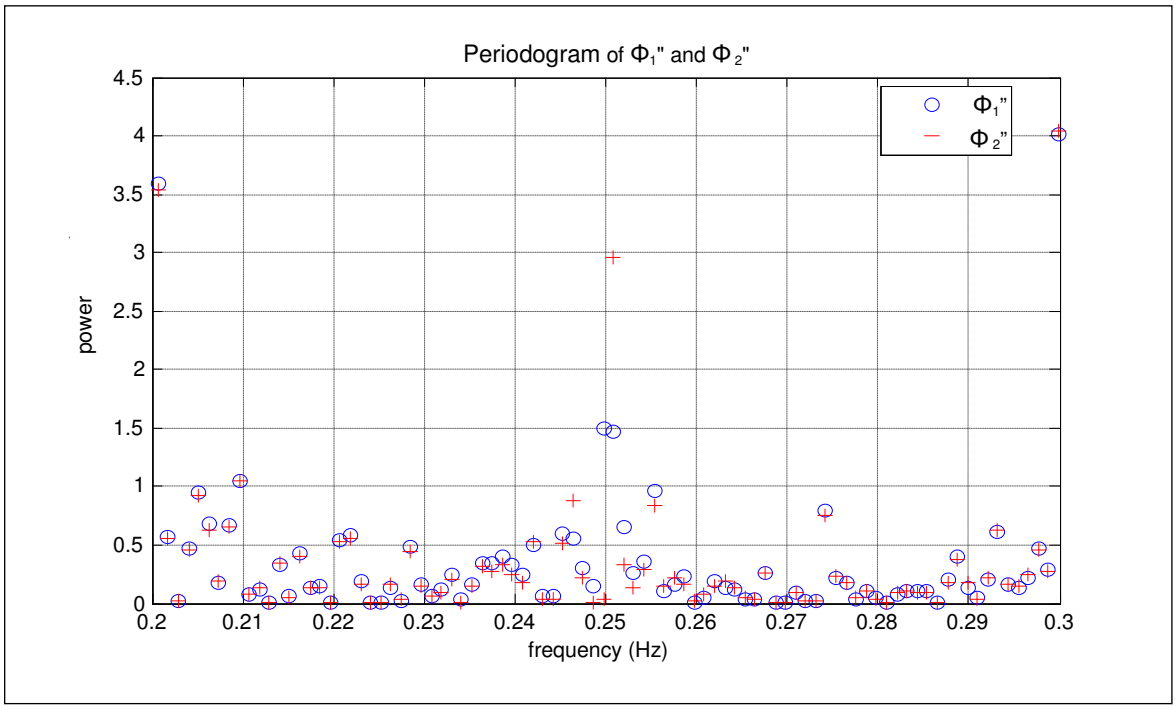

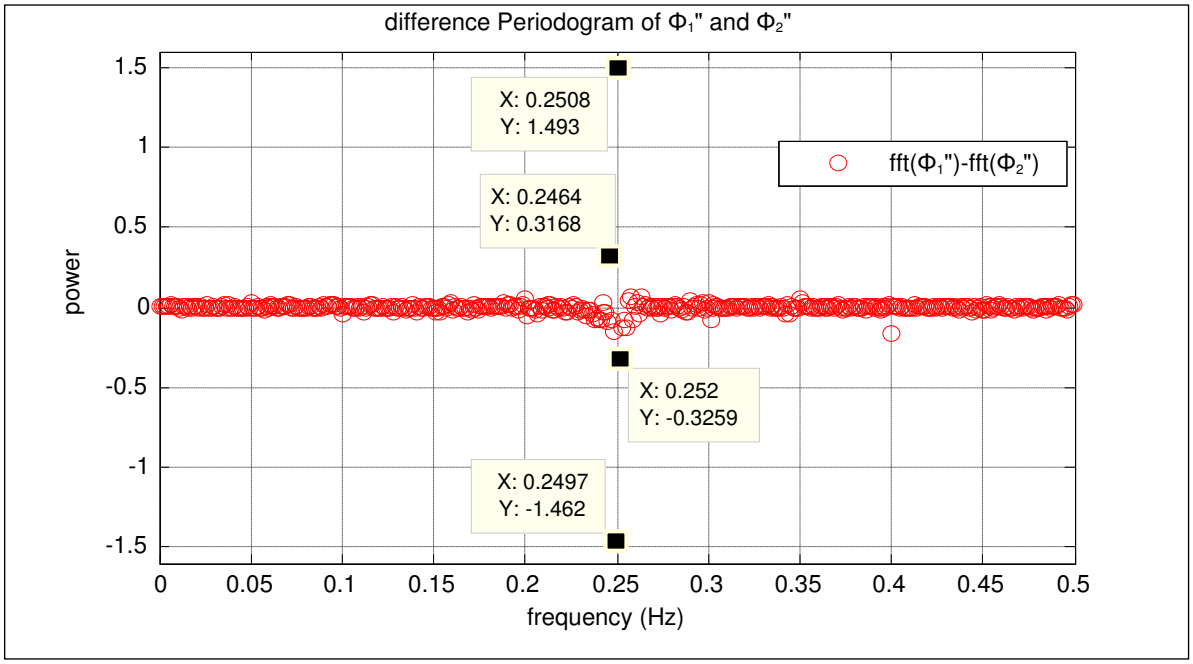

Figure 4. 8 Periodogram of Φ_1" and Φ_2" and their difference (data from WUH2, doy 260 year 2007 PRN3)

The above figure 4.8 is the periodogram of Φ_1" and Φ_2". Close to the frequency 0.25 Hz there are two pairs of points are not matched. But it is still unknown, which carrier phase measurement causes the oscillation.

The three IGS stations, POTM in Potsdam, WUH2 in Wuhan and OBE2 in Oberpfaffenhofen, have same receivers' and antennas' type: AOA BENCHMARK ACT and all of them are maintained by GFZ.

Other stations however with the same receivers Type, antennas Type and Responsible Agency have not the same problem. The reason is not jet clear. And after a discussion in GFZ, the 1 Hz GPS data from those three stations will be not used before the equipments are checked.

4.4 Single difference between satellites

From the above analysis we know the algorithm TurboEdit is not suitable to detect cycle slips in 1 Hz GPS data. And the single difference between satellites will be also tested. Since the orbiting GPS satellites transmit L_1 at higher power than L_2; as a result, the received L_1 signal to noise ratio (SNR) will be better than that for L_2. Spatially, when the GPS satellites are in low elevation position, the noise at L_2 is significantly bigger than the noise at L_1.

Chapter 4 Compare 1 Hz and 0.033 Hz GPS data

When we combine L_1 and L_2, the biggest of the noise in the combination comes from L_2. To take advantage of L_1 signal the between-satellite single difference (one receiver and two satellites) of carrier phases will be more effective to detect cycle slips and outlier. Since the high rate data sampling can represent clearly the high variation in ionosphere delay, troposphere delay, and the most GPS receiver clocks can have high frequency variation, the between-satellite single difference eliminates the GPS receiver clock instability.

Flowing Figures 4.9-12 show us the data from PIE1 doy 260 year 2007

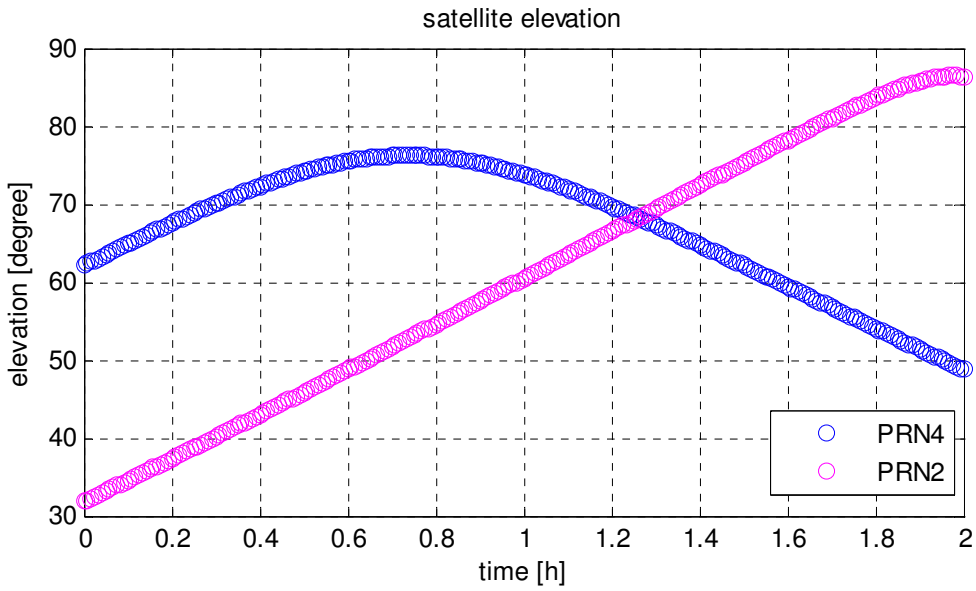

Figure 4.9 Two satellites elevation

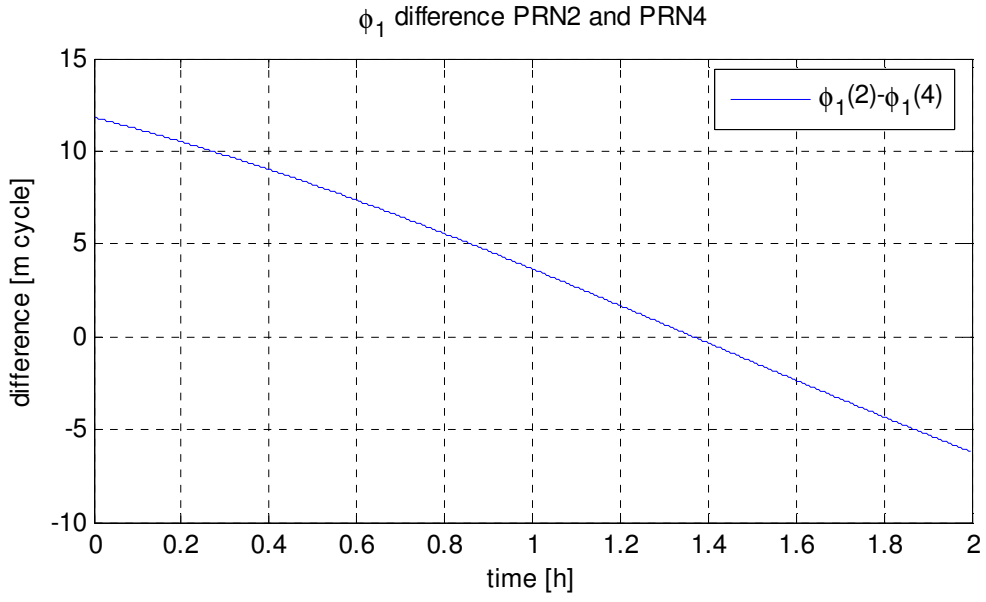

Figure 4.10 Φ_1 single difference between PRN2 and PRN4

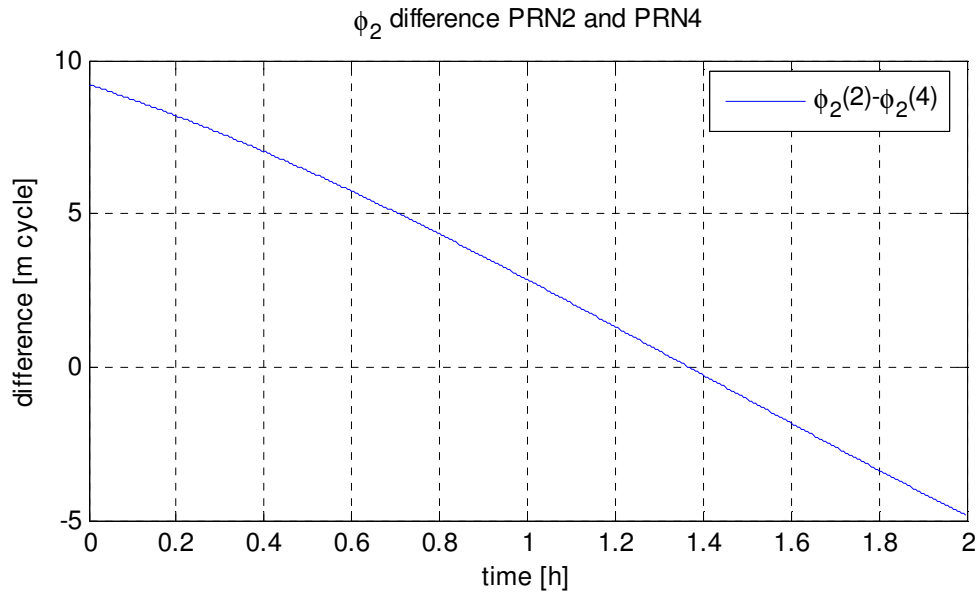

Figure 4.11 Φ_2 single difference between PRN2 and PRN4

The motion of a GPS satellite relative to other GPS satellite can be considered as uniform acceleration. It is the biggest contribution in the carrier phase single difference. Beside it the troposphere and ionospheric delay's difference between observations of two satellites is also a part of the carrier phase single difference. Those effects should be a reasonable smooth function.

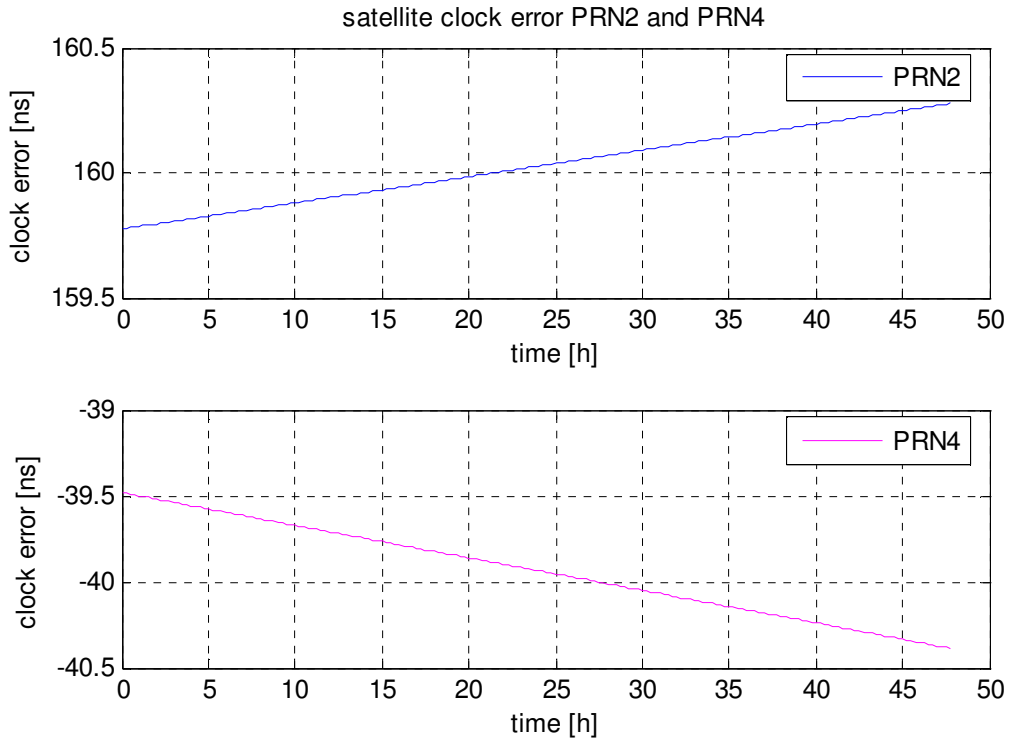

Figure 4.12 Satellites clock error of PRN2 and PRN4 (15 min data from SP3 file)

The Figure 4.12 shows, that the satellite clock error is also a smooth function. The carrier phase single difference includes GPS satellites clock error difference. Since GPS satellites have an atomic clock, and it is much stable.

4.5 Conclusion

From the above analysis, we can get the follow conclusion: Because the precision of the pseudorange measurements in 1 Hz GPS data are not enough for the cycle slips detection, the TurboEdit algorithm can not be used for our purpose. After study the all the combination and difference, we found that the single differences between satellite are very smooth function, when there is no cycle slips occurred. With the single difference between satellites it will be very effective to detect cycle slips.

5. Detection with single differences

Base on the above analysis the single differences are implemented in the preprocessing procedure. In this chapter the computer program will be introduced. Since the goal of this work is to develop computer code for 1 Hz GPS data preprocessing, and like many other famous GPS software (Bernese, EPOS), the preprocessing module in GSEIS software package is also developed in Fortran 90 under Linux.

5.1 Input file and data streams

For the purpose of preprocessing the real time observation data stream L_1 and L_2 should be checked. To find out a reference satellite in possible short time, the satellites' elevations are sorted descending, and under this sequence the reference satellite is searched, which has no cycle slips and has possible little noise in its observations.

Since the rough estimated satellites' elevations are enough for our purpose. The approximate coordinates of GPS receivers can be gotten from the RINEX head file. To calculate elevation we only need the approximate coordinates of GPS satellites in the same coordinate system as GPS receivers. To get the satellites' approximate coordinates there are two ways, one is to compute them from the satellite information in the GPS broadcast ephemeris file; the other way is to interpolate the satellite coordinates directly from IGS products (predicted satellite orbit). Obviously the first way need more time than the second to calculate satellite coordinates, but it requests less communication with analysis centre to get IGS products.

L_1 and L_2	From GPS received row data
GPS satellite position	From IGS products or estimated from GPS broadcast

Table 5.1 Input data for preprocessing

Because the GSEIS software is still in design phase, how to get the GPS satellite position in the preprocessing is still in question. In the current version the GPS satellite position is interpolated from IGS orbit product.

```
*  2007 12 20  9 15  0.00000000
PG01  17400.865583 -19792.566411   3167.196289    173.713380
PG02  -7078.471709  14102.021908  21145.269210    159.777460
PG03   7836.401622 -23180.158410 -10134.872465    160.857400
PG04 -19523.553655   7593.772207  16451.426669    -39.487740
PG05  15978.084914  18235.146514  10745.534785    606.141380
PG06  17458.244004   2435.467297  20052.420923    183.624750
PG07  19040.245384  -1430.493386  18807.728881    -18.888550
```

PG08	-24448.715209	812.570169	-11005.331229	-134.076320
PG09	15729.755304	14465.178097	-16500.558103	101.844530
PG10	56.360738	24534.473623	9621.838377	-179.577430
PG11	-18712.887891	-12473.534991	-14505.123545	26.682960
PG12	12305.971720	22444.411407	7318.287575	-351.926510
PG13	-17653.005267	-499.105950	19727.186544	229.063430
PG14	20962.971259	-14146.107325	-7853.852856	-311.801080
PG15	-32.713806	19235.590100	-18292.197058	-71.005570
PG16	3587.231153	-22248.166212	13994.796083	129.499990
PG17	-21080.229439	13411.783713	-8772.930604	46.190100
PG18	16404.283909	7788.268000	-19327.125977	-218.069100
PG19	888.377785	-18838.906904	-18554.159235	12.921960
PG20	-13851.075637	-20585.781150	9434.657676	124.163800
PG21	26242.758608	5636.866709	-1415.414275	74.983770
PG22	13576.129840	-8144.312873	-21161.182776	205.473080
PG23	-9068.963136	-12097.678352	21755.471983	319.462250
PG24	20872.208043	13045.647310	9770.653875	55.442720
PG25	-24870.449589	-7264.455352	5813.570416	492.783400
PG26	-3313.408035	19635.754750	-17738.816070	131.233000
PG27	-26330.982458	-4079.130036	-298.915788	155.361150
PG28	-14326.720425	4465.250189	-21554.254819	-12.325930
PG30	16639.154589	13166.449089	15705.174557	56.780570
PG31	17014.616976	-9267.217571	18409.872368	-2.091330

Table 5.2 IGS orbit product in SP3 format

The first line is the GPS time of the prediction. In the following lines there is the satellites' number, components of position in meter and clock bias in nanosecond.

5.2 Structure of the software

In every second the program gets GPS observations from the NTRIP data streaming, after processing the observations, which are tested as cycle slip or outlier, are flagged, and the flags will be outputted for the parameter estimation.

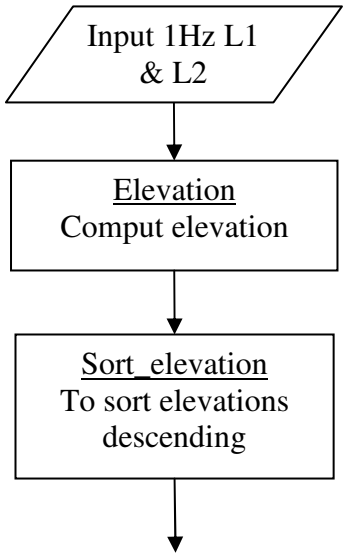

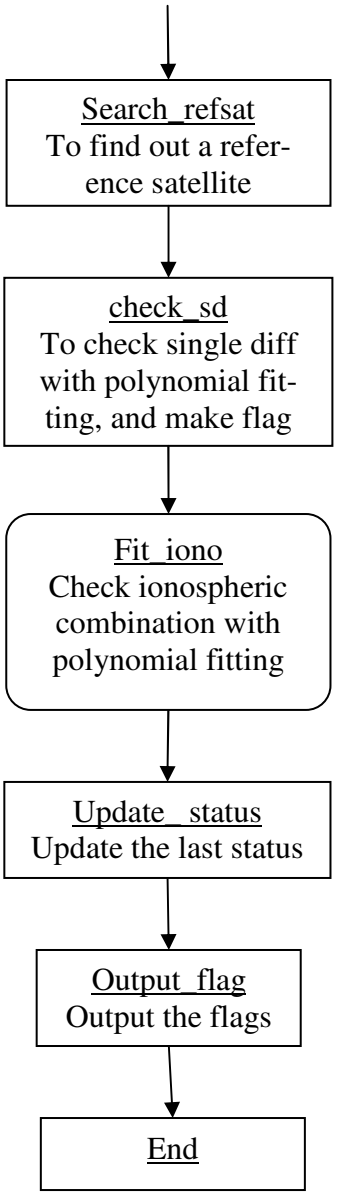

Figure 5.1 Main program diagram of chn_filter

During the preprocessing the last 10 seconds carrier phase observations from L_1 and L_2 are always updated, which are prepared for the next polynomial fitting. Every second the program estimates the newest coefficients for all satellites' observation, it can deal with high ionosphere activity very effectively, and it is flexible to change reference satellites. Compared to radio signal the GPS signal is very weak, receiver can loose lock GPS satellite signal for a short time, from several seconds to several minutes, after that the ambiguity is still possibly unchanged. For this case the last estimated polynomial coefficients are also saved with reference satellite number and reference time together for every satellite. When the signal loss is longer than 10 minutes, the saved polynomial coefficients of the satellite are set invalid.

In the program there are two important steps, initialization and single difference checking.

a) In initialization phase, if the reference satellite can not be found, the program must wait for enough observations without cycle slips or outlier.

b) In cycle slip detection, the last 10 single differences between satellites are fitted with a quadrate polynomial, which is estimated with the least squares method.

5.3 Initialization phase

To make single difference between satellites we need a reference satellite, which has low noise in observations L_1 and L_2 at the last 10 epochs. This means that after the program start or after a long time without GPS data, it needs at least 10 seconds to initialize.

To save time in this phase the program searches for reference satellite in descending order of the satellites elevations' angles. Since the GPS observations from higher elevation angle have less noise than those from lower elevation. And we do not have to check L_1 and L_2 separately but only the ionospheric combination from L_1 and L_2.

When a satellite has 10 available observations in L_1 and L_2 in the last 10 seconds, and after polynomial fitting of the ionospheric combinations the standard deviation RMS is also smaller than 0.3 cycles. Then we extrapolate the estimated polynomial to current epoch. If the difference between the ionospheric combination in the received current epoch and the extrapolated value is smaller than 0.6 cycles, then this satellite is suitable as reference satellite for the current epoch. Otherwise the next satellite will be tested. When we can not find a reference satellite after checking all of satellites, the program has to wait until enough observations without cycle slip or outlier are received.

When a GPS satellite arises, the observation in first 5 epochs will not be flagged. Then the program will try to fit them with 2 degree polynomial. If the polynomial fitting is successful, then the initial phase of the GPS satellite data is finished, otherwise the program must wait for more observations from this new GPS satellite.

5.4 Polynomial Fitting

After the successful initialization the L_1 and L_2 single difference between reference satellite and other satellites in the last 10 seconds are calculated. They will be checked for cycle slips separately.

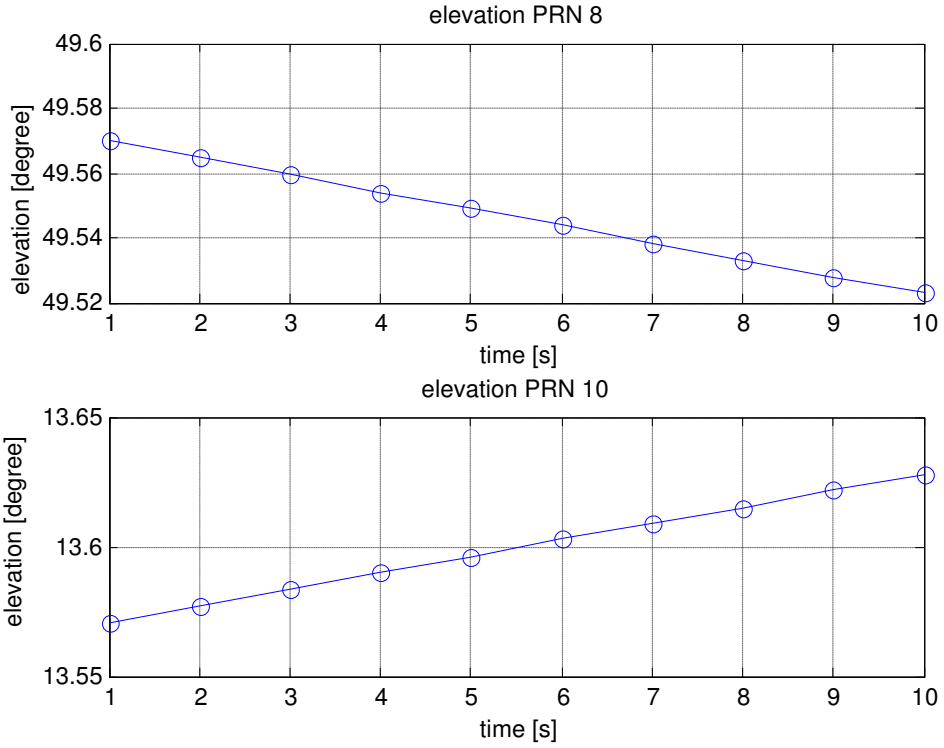
elevation PRN 8
elevation [degree]
49.6
49.58
49.56
49.54
49.52
1
2
3
4
5
6
7
8
9
10
time [s]
elevation PRN 10
elevation [degree]
13.65
13.6
13.55
1
2
3
4
5
6
7
8
9
10
time [s]

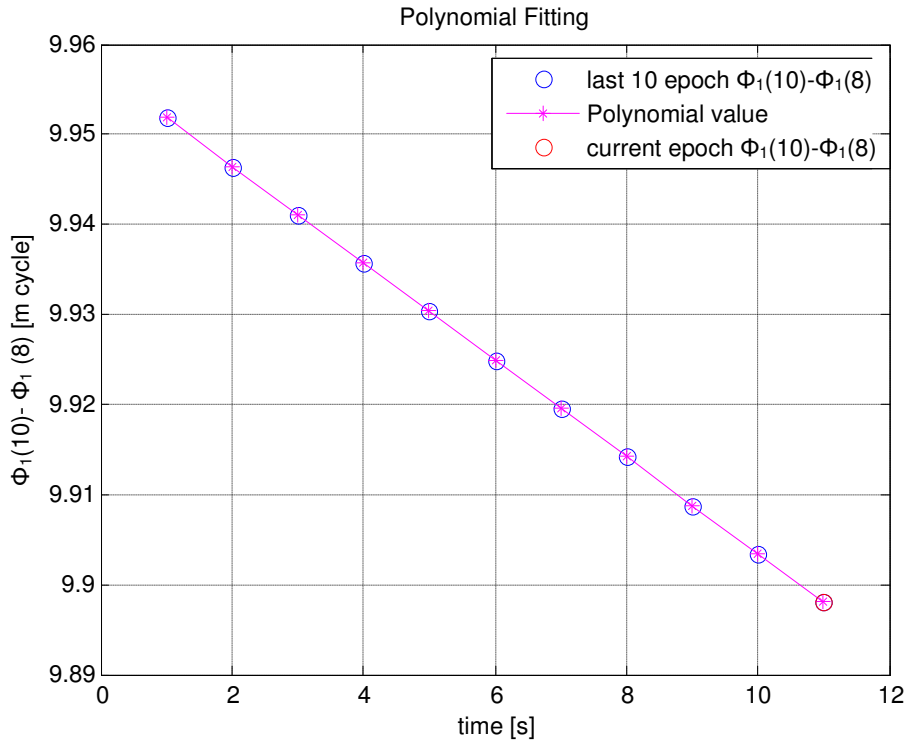
Polynomial Fitting
last 10 epoch Φ1(10)-Φ1(8)
Polynomial value
current epoch Φ1(10)-Φ1(8)
Φ1(10)- Φ1 (8) [m cycle]
9.96
9.95
9.94
9.93
9.92
9.91
9.9
9.89
0
2
4
6
8
10
12
time [s]

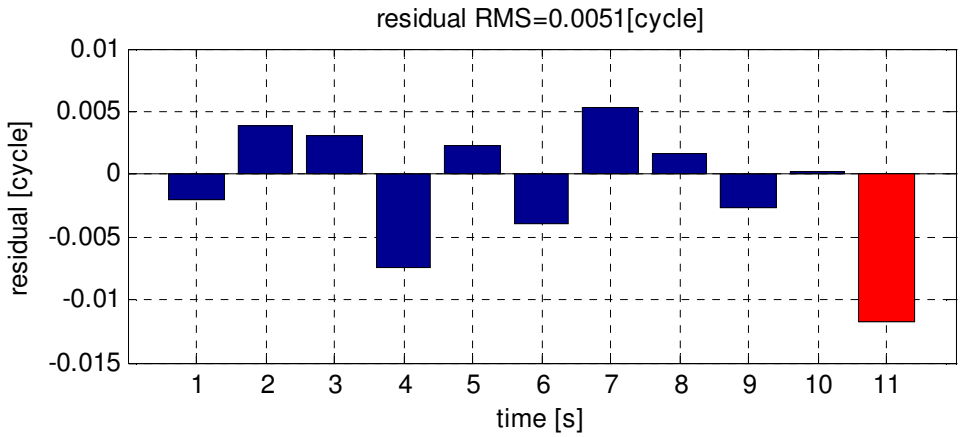

Figure 5.2 Elevation angles of two satellites (top) L_1 single difference polynomial fitting (middle) and residual (bottom)

In Figure 5.2 L_1 differences of the last 10 epochs between the reference satellite 8 and satellite 10 is fitted with a 2-order-polynomial. The RMS (Root Mean Square) shows the quality of the last 10 epochs L_1 and the estimated polynomial. From the residual of the current epoch we can find out a cycle slip.

When there are some outliers or observations with big noise in the last 10 epochs, they will not be used in the polynomial fitting. For this reason the flags of the last 10 epochs' observations are also saved in a matrix, 1 for observations with big noise or outlier, 0 for good observations. But at the initialization phase we give 1 to the flags of the last 10 epochs without checking. This means, the polynomial fitting should be able to estimate coefficients robustly. In this program when the RMS is too big after 2 order polynomial fitting, and there are still more than 5 good observations in the last 10 epochs, then a one order polynomial is estimated and the data with the largest residual is detected as outlier, with rest data the next try of 2 order polynomial fitting begins.

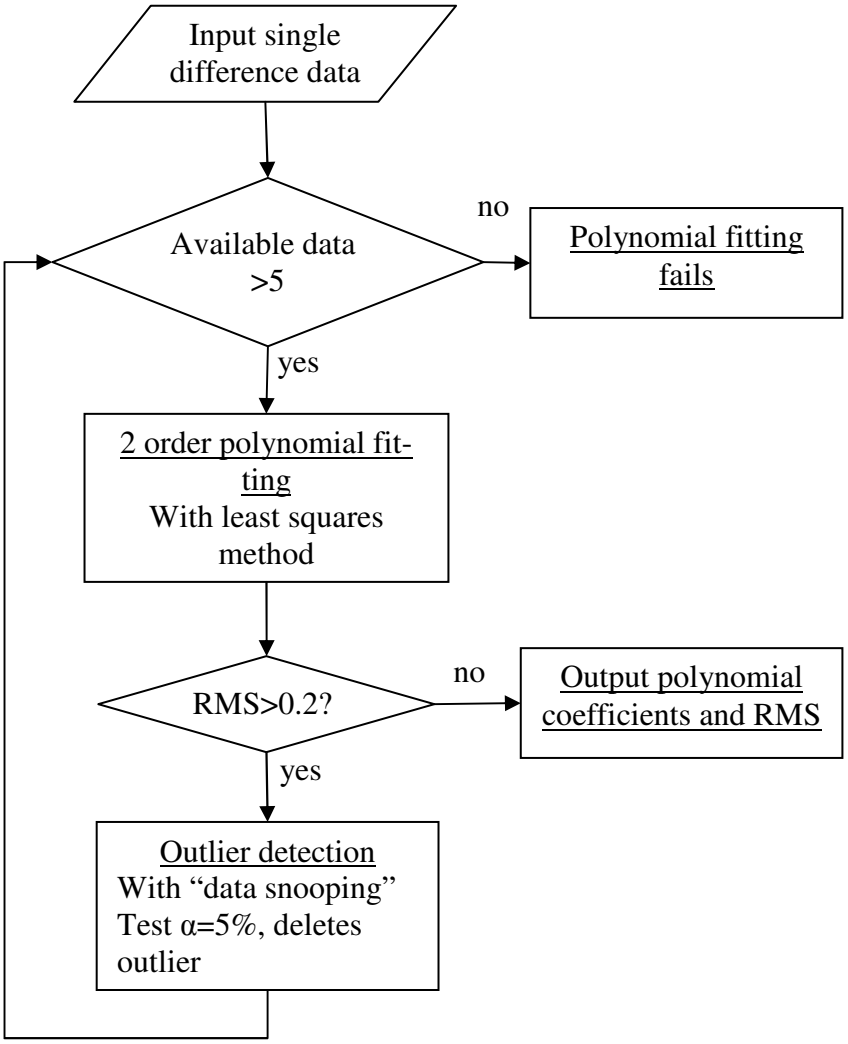

Figure 5.3 Outlier detection in polynomial fitting

Figure 5.3 shows polynomial fitting. If the polynomial fitting fails, the program will wait for next epoch data, until polynomial fitting is successful.

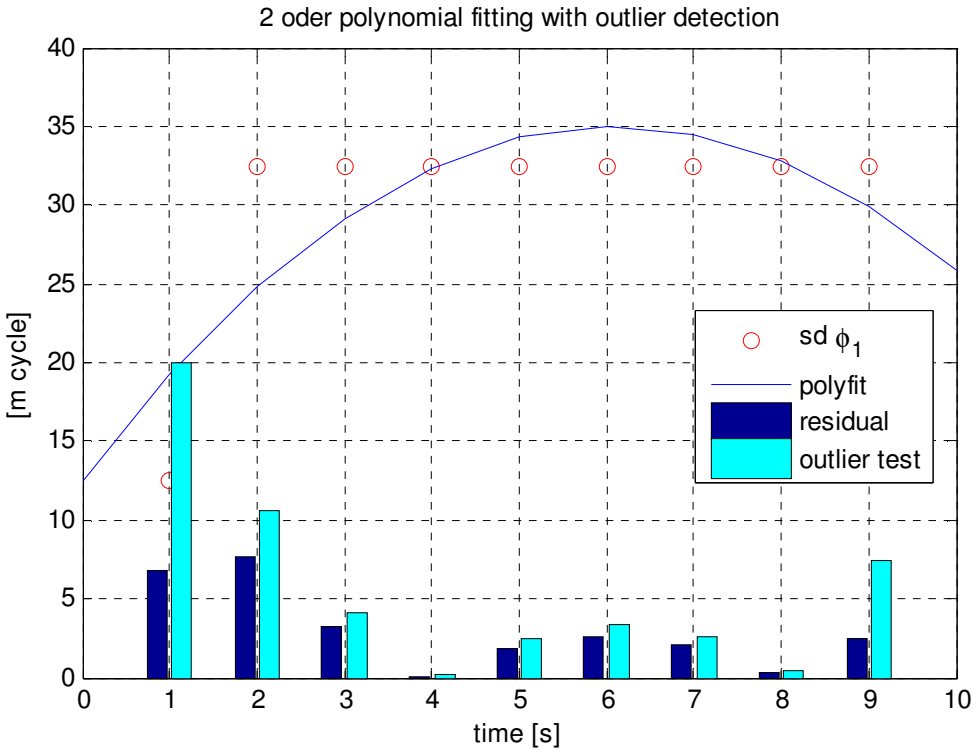

Figure 5.4 outlier detection with 2 order polynomial fitting (sd: single difference)

In this example there are two outliers in time 1 and 8. They will be detected by outlier test POPE.

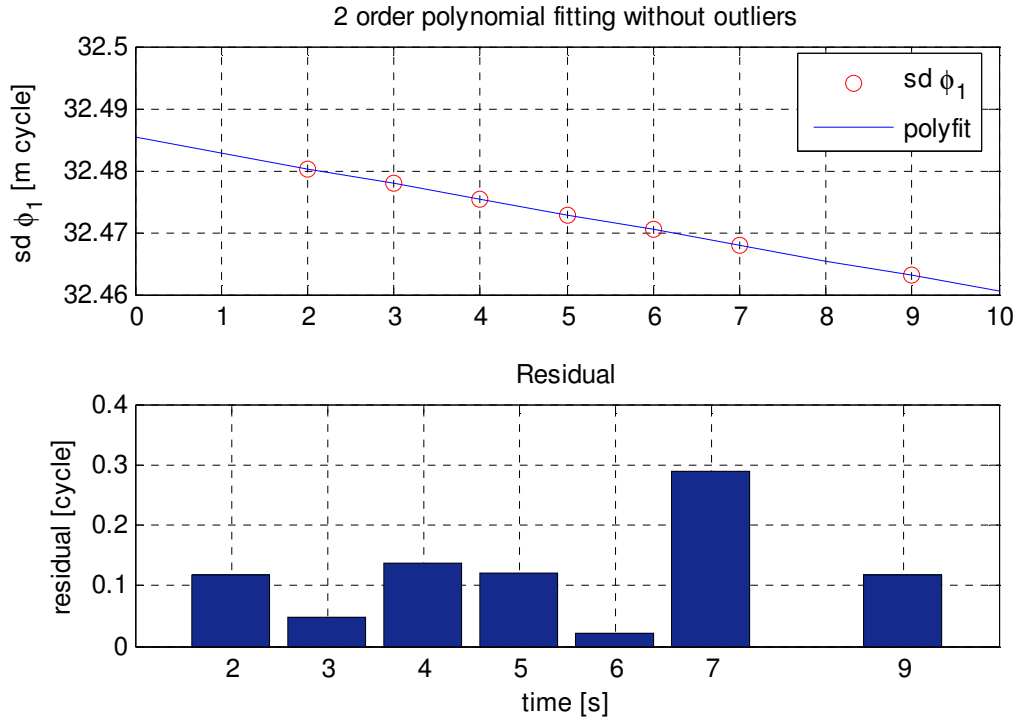

Figure 5.5 2 order polynomial fitting without outliers

Because the last 10 epochs with outliers happen often in initial phase, the outliers must be cleared before polynomial fitting.

5.5 Single difference checking

When the single difference between the reference satellite and an other satellite in the last 10 epochs is fitted with a 2 order polynomial successfully, or the last successful polynomial fitting is not 10 minuses earlier than current epoch, then the polynomial is extrapolated to current epoch to get a model value; the single difference of current epoch is required to lie within 0.6 cycle of the extrapolated value.

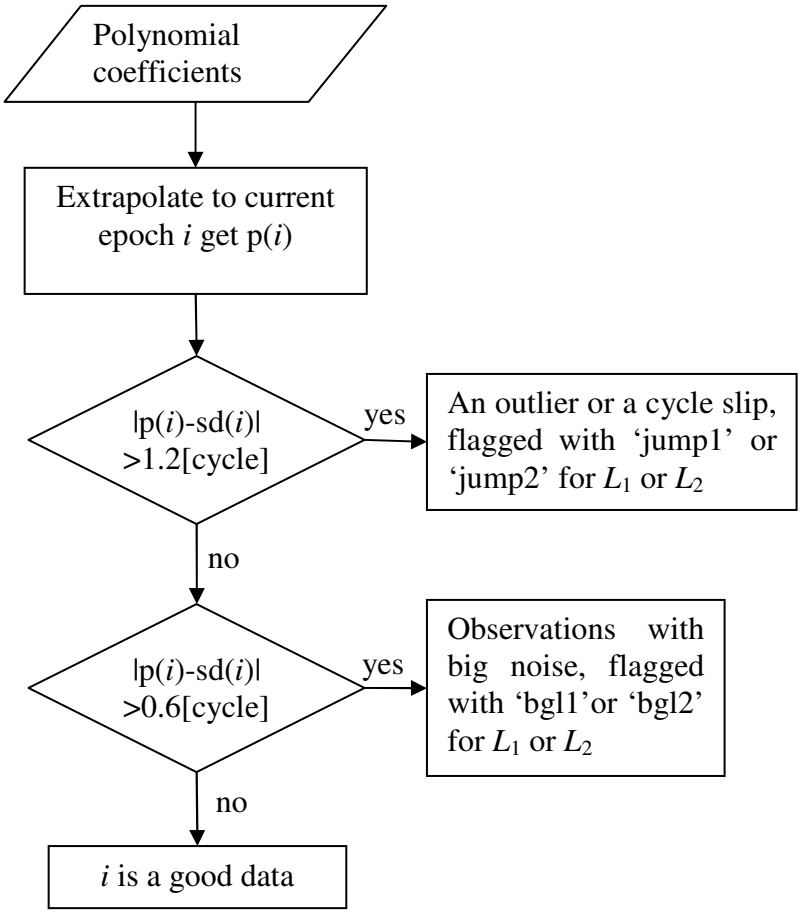

Figure 5.6 check current epoch

Carrier phase L_1 and L_2 should be checked separately. After the check there are 3 possible results: 'jump', 'big noise' and 'good data'. For the result 'big noise', there is possible one cycle slip occupied. One cycle slip in carrier phase L_1 or L_2 can causes bigger than 3 cycles jump in their ionospheric combinations. Thus we can check the ionospheric combinations with polynomial fitting, when a 'big noise' is flagged in carrier phase L_1 or L_2.

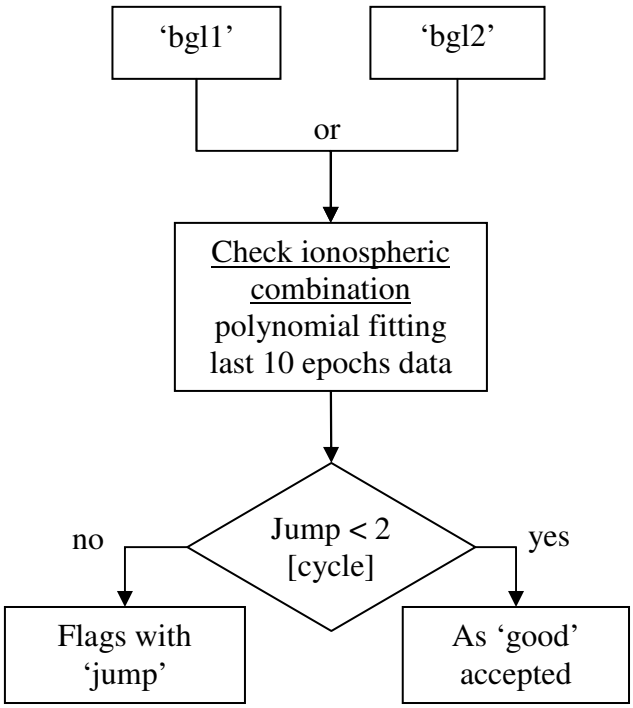

Figure 5.7 Check big noises with ionospheric combination

Because of its smaller variation the ionospheric combination is very effective to check the carrier phase with big noise.

5.6 Results

To test this program the 6 days data from about 110 IGS GPS stations are downloaded and checked. Results are in the following figures.

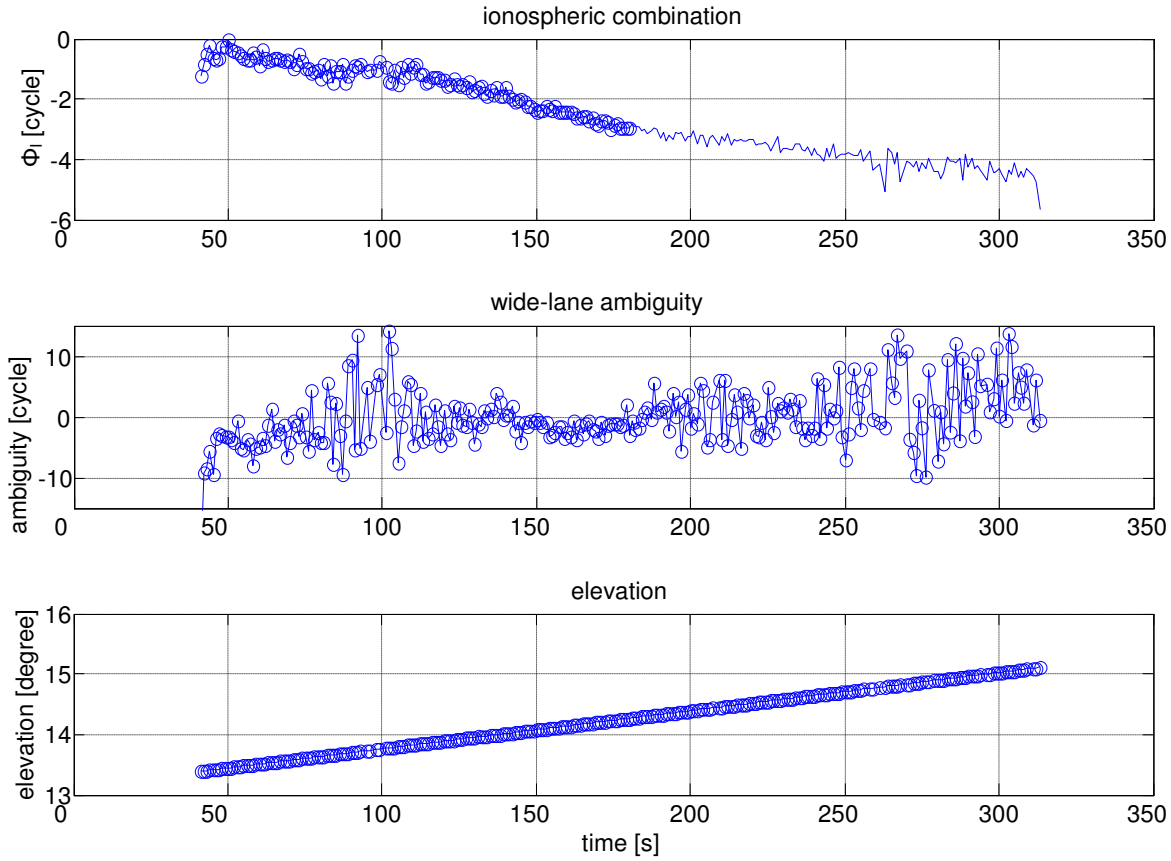

Figure 5.8 Variations in combination of 1 Hz GPS data

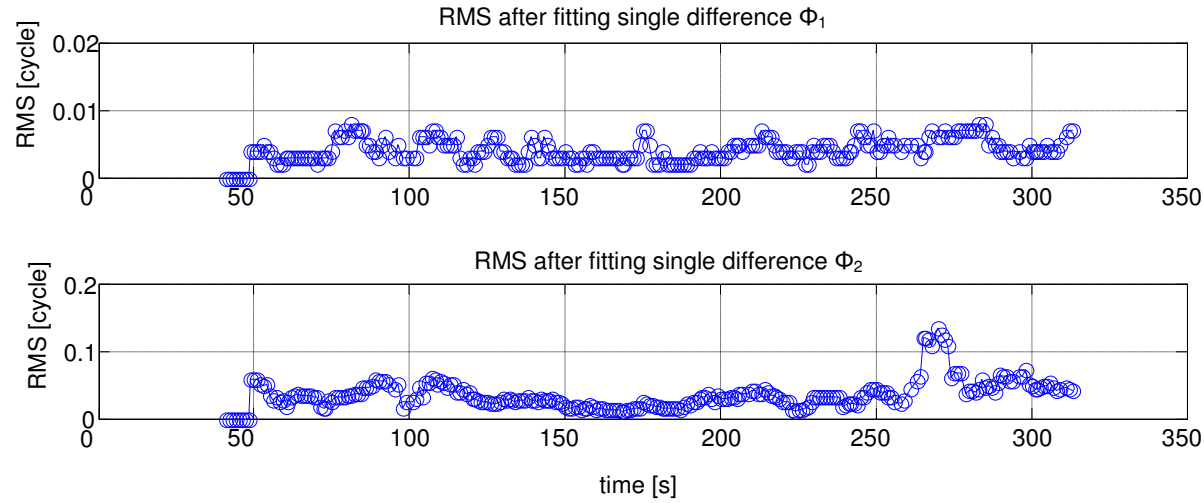

Figure5.9 RMS after polynomial fitting of 1 Hz GPS data

In both figures 5.8-9 we used the data from ULAB doy 260 year 2007 PRN11. The same 1 Hz GPS data is checked with difference method. In the Figure 5.8 the ionospheric combinations have a large than 1 cycle jump at time = 264; it can be possible that both of L_1 and L_2 have one cycle slip. And from the wide-lane combinations we can not get any help. In this case the two combinations are not suitable to detect cycle slip. As discussed in the previous chapter, which the RMS of polynomial fitting identifies, the carrier phases quality in the last 10 ep-

ochs. From the figure 5.9 the RMS in L_2 is about 10-20 times bigger than the RMS in L_1, and the bigger variation in L_2 is the cause of the variation in ionospheric combination.

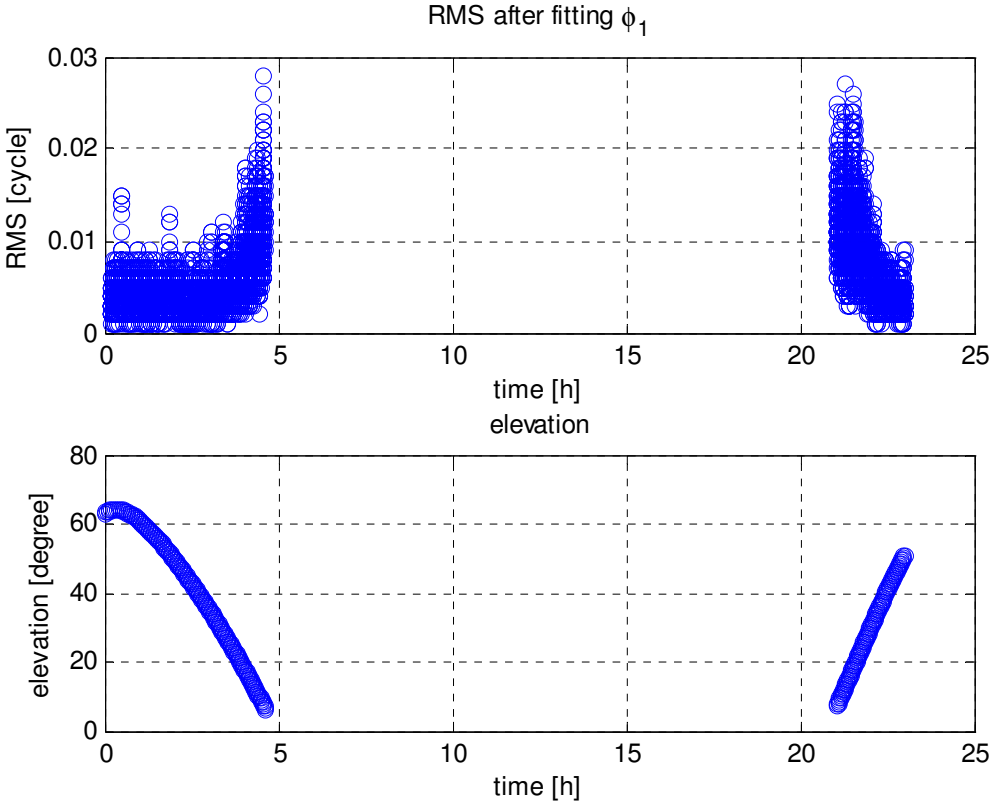

Figure 5.10 RMS and elevation angle

In figure 5.10 the 1 Hz GPS data of the station PIE1 in doy 260 year 2006 PRN1 are used. The experiments show a high negative correlation between satellite elevation angle and RMS of polynomial fitting. In these experiments the cutoff elevation angle is 7 degrees. Even at low elevation angle the RMS are still small enough to check out the cycle slips with only one cycle.

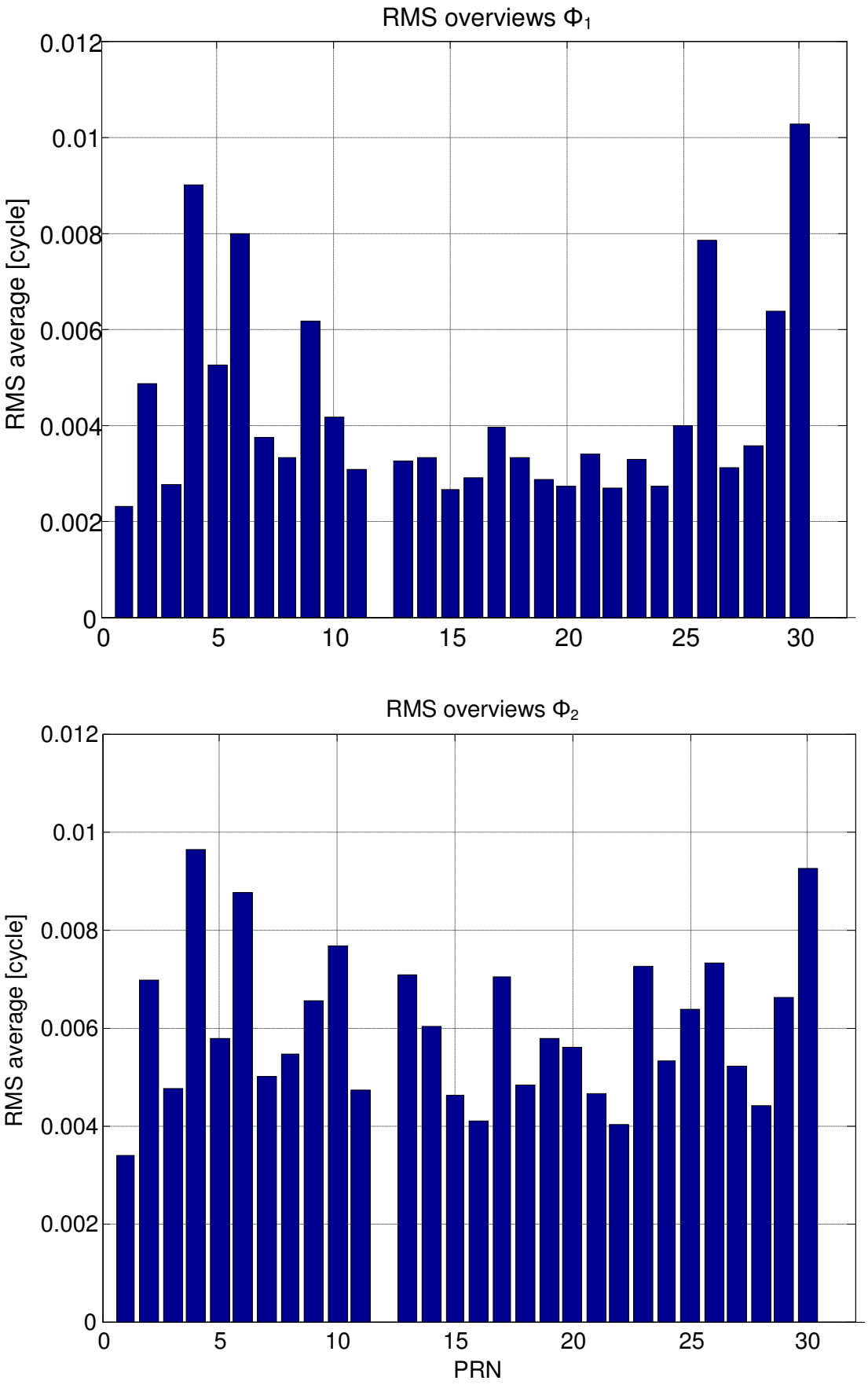

Figure 5.11 RMS after polynomial fitting for all satellites in one doy

doy year	Elevation >=7°	good Φ_1	%	good Φ_2	%
100 2006	733461	731375	99.7	731375	99.7
200 2006	706329	703989	99.7	703988	99.7
260 2007	683967	682538	99.8	682538	99.8
320 2007	758406	756574	99.8	756575	99.8

Table 5.3 Rate of good data after checking (station: PIE1)

Table 5.1 is the checking result of the 1 Hz GPS data from IGS station PIE1.The numbers in Table 5.1 the 2nd column are the sums of the observations with higher than 7 degrees elevation in the test doy for all satellites. And in the 3rd and 4th column there are the sums of carrier phase observation without cycle slip or outlier after Channel_Filter check. The most lost data are caused by initialization phase.

After checking 6 days of about 110 IGS stations with the program Channel_Filter, the average rate of good data Φ_1 is 99.59 %, and for Φ_2 it is 99.55 %.

6. Analysis of single frequency receivers

Since single frequency code/carrier phase GPS receivers are less expensive than dual frequency receivers, and many single frequency solutions exhibit equivalent accuracy as those obtained from dual-frequency observations, single frequency receivers become more popular nowadays. GFZ plans to build a GPS network with 1500 single frequency receivers in Germany for meteorology research. Here the receiver clock bias and carrier phase measurement of three single frequency GPS receiver (GARMIN, THALES and NOVATEL) are tested and compared. During which the Channel_filter is used.

6.1 Determination of reference satellite

For single-frequency carrier phase GPS receivers it is impossible to determine a reference satellite with the ionospheric combination. Since GPS observations from higher elevation angle have less noise than those from lower elevation. Here we set the satellite with the highest elevation as the reference satellite.

6.2 GARMIN (GPS 17-HVS)

The first tested GARMIN (GPS 17-HVS) is a low cost single frequency GPS receiver, which outputs raw pseudorange and carrier phase data. It can track and use up to twelve satellites with a default data rate of 1 Hz in the Garmin proprietary format. After conversion to standard RINEX format, we get:

08 01 21 01 13 12.2044286 0 7G08G28G18G09G26G17G15 -514001149.557 3566712596.295 42.000 -516342019.704 3839321302.908 51.000 -515349264.667 4093958455.476 36.000 -516401070.332 4145103917.072 47.000 -517824036.326 3849405565.825 52.000 -515671088.193 4144350802.482 50.000 -517834638.842 3862259609.821 53.000
C_1 **Φ_1** **S_1**

Table 6.1 One epoch 1Hz GPS data from GARMIN (in RINEX form)

Usually the distance between a satellite and a site is more than 20,000 km, in the above received observations the C_1 is negative. This means that the clock of GARMIN GPS 17-HVS

has big offset. Before we begin to preprocess the 1Hz GARMIN GPS data, the clock offset must be estimated. Here we attempt to calibrate the receiver clock using GPS broadcast ephemeris.

$$C_1^{\,k} = \rho^k + dt^k + dt + I^k + T^k \tag{6.1a}$$

$$dt + I^k + T^k = C_1^{\,k} - \rho^k - dt^k \tag{6.1b}$$

I^k : ionospheric delay

T^k : troposphere delay

ρ^k : distant between satellite and site, calculated from GPS broadcast and the known site coordination

dt^k : satellite clock error, calculated form GPS broadcast

dt : receiver clock error

k : satellite index

From equation (6.1b) we can get the sum of receiver clock error, ionospheric and troposphere delay.

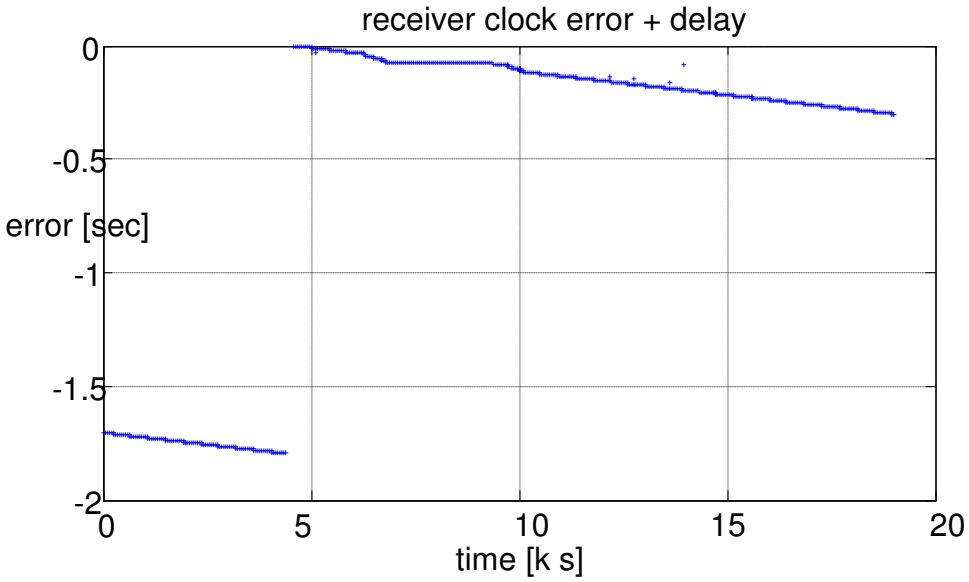

Figure 6.1 Receiver clock errors, ionospheric and troposphere delay

At time=4.6 [m s] the GARMIN receiver clock was synchronized with an atomic clock. The GARMIN receiver clock has not only offset, but also drift. After correcting the receiver clock error and regardless of the delay the Channel_filter is run to check the RMS after polynomial fitting.

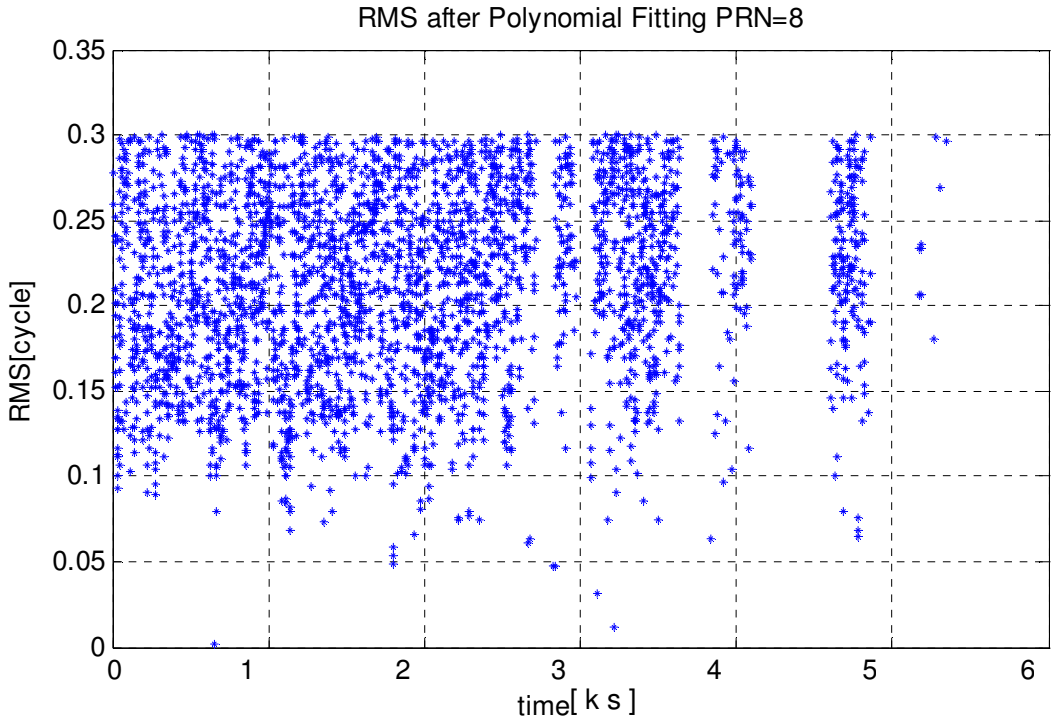

Figure 6.2 RMS for GARMIN 1 Hz data checking

The RMS of GARMIN carrier phase polynomial fitting is disorderly, and it is impossible to detect a cycle slip. GARMIN (GPS 17-HVS) can not be used for GPS carrier phase observation.

6.3 THALES (AC-12)

The THALES AC12 receiver provides raw data output with carrier phase measurements. With THALES(AC-12) 3 days of 1 Hz GPS data have been generated. After checking raw data, there is no conspicuous offset and drift of the receiver clock.

With the program Channel_filter the RMS of polynomial fitting will be checked.

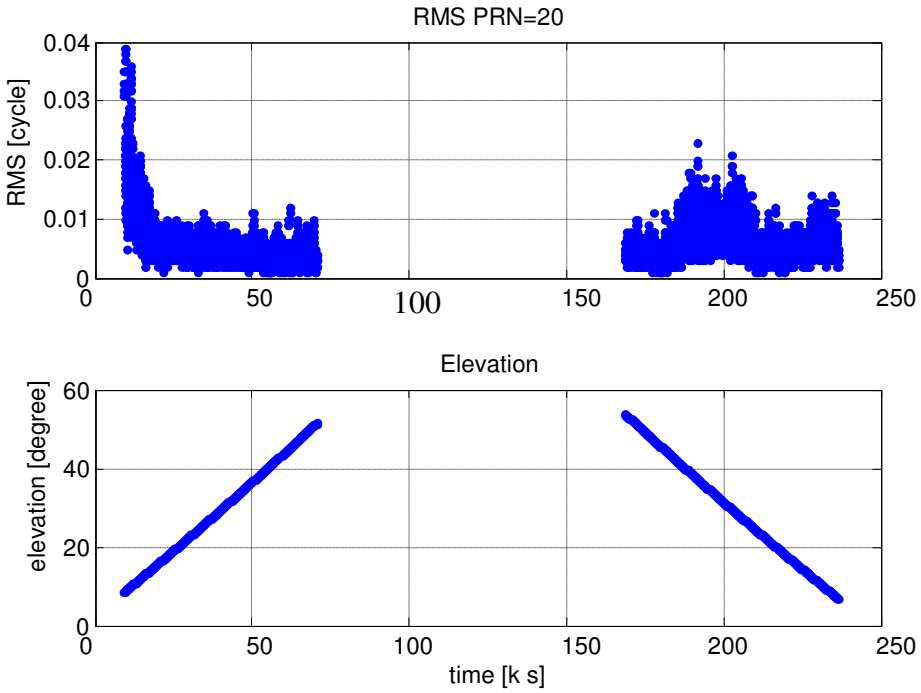

Figure 6.3 RMS for THALES 1 Hz GPS data checking

In the gap of Figure 6.3 the PRN20 was taken as reference satellite.

doy year	Elevation >=7°	good L1	%
034 2008	796653	794080	99.7
035 2008	798109	797403	99.9
036 2008	796704	795777	99.9

Table 6.2 Rate of good data after checking (THALES)

This study showed that the quality of the GPS carrier phase measurements of the single-frequency THALES (AC 12) is equivalent to the dual-frequency GPS receiver.

6.4 Novatel (smart antenna^{TM})

The SMART ANTENNA™ integrates a GPS receiver and an antenna; it features 12-channel code and carrier phase tracking for improved positioning accuracy and reliability. It provides position, velocity, and time (PVT) output at rates up to 5 Hertz or raw carrier phase measurement data at rates up to 10 Hertz. [novatel]

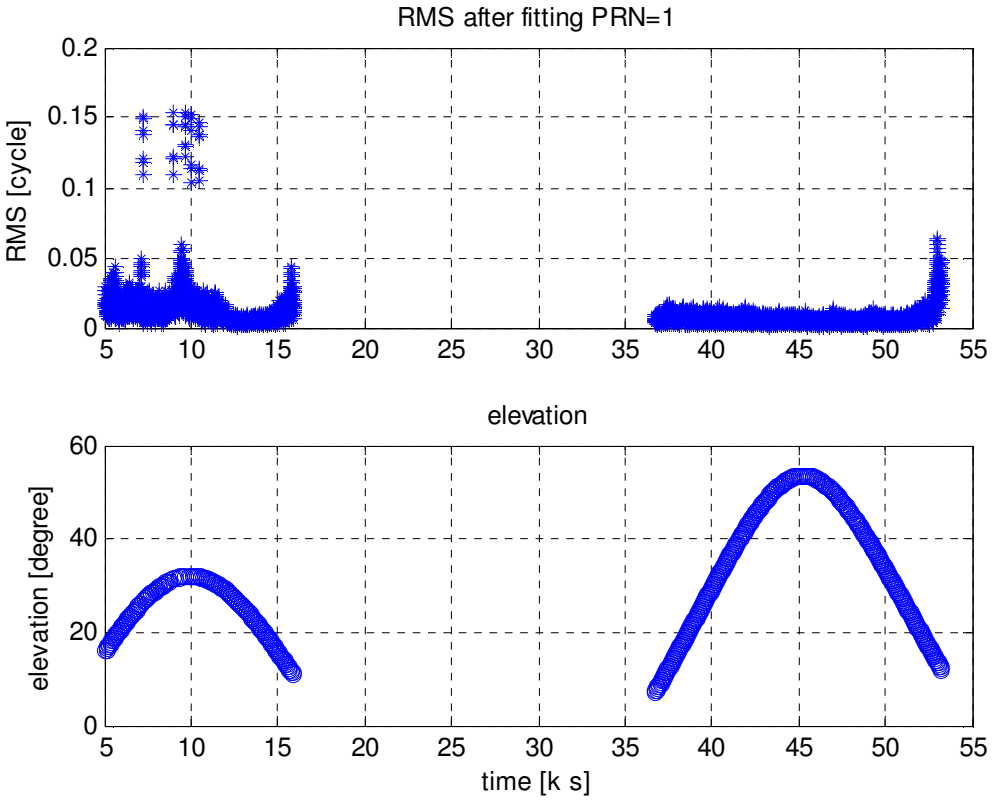

Figure 6.4 RMS for Novatel 1 Hz GPS data checking

The RMS of Novatel has some jumps at the satellite at big elevation, but it is correlated with elevation.

doy year	Elevation >=7°	good L1	%
054 2008	112629	112310	99.7
058 2008	796704	795777	99.65

Table 6.3 Rate of good data after checking (Novatel)

At the doy 054 there were only 4.25 hours observation data.

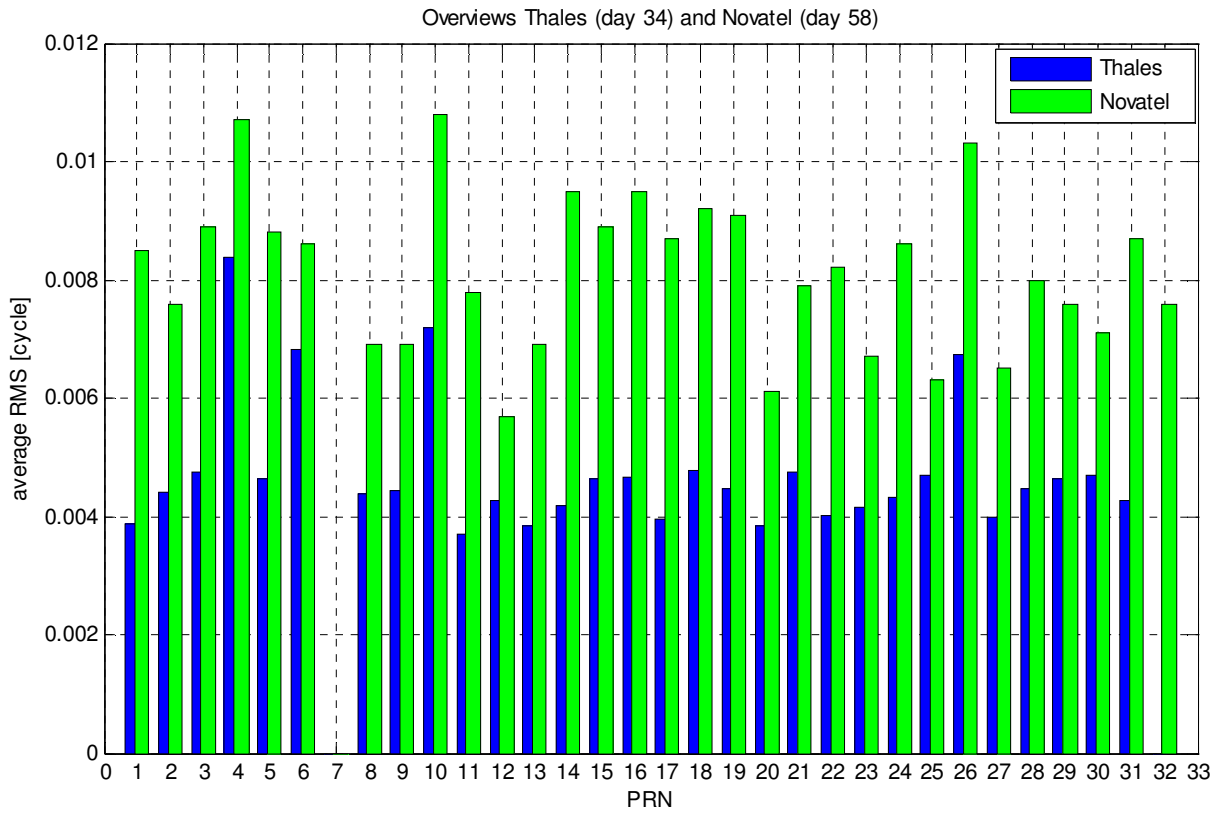

Figure 6.5 RMS after polynomial fitting for all satellites (THALES & NOVATEL)

Comparing THALES with NOVATEL the noise in the THALES received GPS data is smaller than in NOVATEL received GPS data.

7. Summary and conclusion

a) In this thesis a new 1 Hz GPS data preprocessing method for real time applications is proposed and implemented in Fortran 90. The preprocessing module, Channel_filter will be used in GSEIS project to detect cycle slips and outliers in 1Hz GPS data stream. Because the method based on PPP real-time positioning is used in GSEIS project, the preprocessing should be able to be used for single GPS station.

b) Currently the algorithm TurboEdit is used publicly in PPP preprocessing for single GPS station. After study the TurboEdit algorithm and EPOS software the new method Channel_filter and its FORTRAN software was developed to detect cycle slip and outlier in real time 1 Hz GPS data. The Channel_filter algorithm is documented by many figures in Chapter 5.

For the examination six days 1 Hz dual frequency GPS data was downloaded from IGS data center and simulated as real-time data stream. In the TurboEdit algorithm there are two combinations, ionospheric and wide-lane combination, which were used for cycle slip or outlier detection. During the examination of the GPS data it was found that the 1 Hz GPS data pseudorange measurements are less precise then the 0.033 Hz GPS data. And the wide-lane ambiguity has very large scatter, and can not be used to detect cycle slips or outliers. Because the cycle slips can occur in L_1 and L_2 concurrent in different value, at least two combinations are need to detect cycle slips in L_1 and L_2 other effective detection will be found out to take place of wide-lane combination.

c) Since the GPS satellites transmit L_1 at higher power than L_2; as a result, the received L_1 signal has less noise than L_2. To take advantage of the L_1 signal the between-satellite single difference (one receiver and two satellites) of carrier phases are a better choice. With this idea the Channel_filter algorithm is developed. In the Channel_filter program there are three steps to detect cycle slip or outlier:

- Find a reference satellite with enough good observations in the last 10 epochs.
- Compute the last 10 epochs L_1 and L_2 single differences between the reference satellite and the other satellite, and then fit a second-order polynomial to the differences.
- Extrapolate the second-order polynomial to the current epoch, and check the residuals. If a residual is bigger than a certain limit, possibly there is cycle slip or outlier in the current epoch.

d) To make a successful detection the RMS of the second-order polynomial fitting should be small enough to detect one cycle slip. In a test with the 6 days 1 Hz GPS data of 110 stations the calculated RMS are less than 0.1 [cycle] for Φ_1 and 0.2 [cycle] for Φ_2. It is easy to check out one cycle slip or outlier with so small RMS.

e) Since single-frequency code/carrier phase GPS receivers are applied in many real-time projects, in this thesis the 1 Hz GPS data of three single frequency GPS receivers GARMIN, THALES and NOVATEL are checked with Channel_filter.

- The GARMIN GPS receiver clock has a drift about 1.7 second/day, and the carrier phase measurements are irregular, and can not be applied for positioning.
- The THALES and NOVATEL GPS receiver exhibit equivalent carrier phase observations as due frequency GPS receiver.

References

Blewitt, G. “An Automated Editing Algorithm for GPS Data”. Geophys. Res. Lett.,17(3), 199-202, March 1990.

Gao, Y. and Chen, K. “Performance Analysis of Precise Point Positioning Using Rea-Time Orbit and Clock Products.” Journal of Global Positioning Systems, Vol. 3 No. 1-2, pp. 95-100. 2004.

Garmin. Germany. GPS-Module GPS 17-HVS. http://www.garmin.de/geraete/gps_mause. php. Accessed April, 2008.

GDC (GNSS Data Center). Germany “NTRIP Networked Transport of RTCM via Internet Protocol” http://igs.bkg.bund.de/index_ntrip.htm. Accessed February, 2008.

Ge, M. Gendt, G., Dick, G., F.P Zhang, and Rothacher M., A new data processing strategy for huge GNSS global networks, Journal of Geodesy, Vol.80, pp199-203, DOI 10.1007/s00190-006-044-x, 2006

IGS. “IGS Real Time Working Group (RTWG)” http://www.rtigs.net/. Accessed February, 2008.

Kedar, S. “The effect of the second order GPS ionospheric correction on receiver positions”, Geophys. Res. Lett., 30(16), 1829 2003.

Rothacher, M.“Satellitengeodäsie 1 (Einführung in GPS)”. Technische Universität München. 2005.

NASA. U.S. High rate GPS data. ftp://cddis.gsfc.nasa.gov/gps/data/highrate/. Accessed February, 2008.

NIMA. SP3 Format Description. http://164.214.2.59/GandG/sathtml/sp3format.html. Accessed February, 2008.

Novatel. “Smart antenna”. http://www.novatel.com/products/smart.htm. Accessed April, 2008.

Rothacher, M. et al. “G-SEIS Proposal of GeoForschungsZentrum Potsdam” 2006.

Thales. “Thales Navigation AC12 Carrier Phase OEM GPS Receiver Sets Performance Standard”. http://www.thalesnavigation.com/. Accessed April, 2008.

Keller, W. “Observation Techniques in Satellite Geodesy”. 64-67. Universität Stuttgart. 2005.

Witchayangkoon, B. “Elements of GPS Precise Point Positioning”. M.Sc.Thesis. the University of Maine. 2002.